

On the dynamics of mean-field equations for stochastic neural fields with delays

Jonathan Touboul

The Mathematical Neuroscience Laboratory, Collège de France, Center for Interdisciplinary Research in Biology (CIRB) and INRIA Paris, BANG Laboratory, 11 place Marcelin Berthelot, 75005 Paris, France

Abstract

The cortex is composed of large-scale cell assemblies sharing the same individual properties and receiving the same input, in charge of certain functions, and subject to noise. Such assemblies are characterized by specific space locations and space-dependent delayed interactions. The mean-field equations for such systems were rigorously derived in a recent paper for general models, under mild assumptions on the network, using probabilistic methods. We summarize and investigate general implications of this result. We then address the dynamics of these stochastic neural field equations in the case of firing-rate neurons. This is a unique case where the very complex stochastic mean-field equations exactly reduce to a set of delayed differential or integro-differential equations on the two first moments of the solutions, this reduction being possible due to the Gaussian nature of the solutions. The obtained equations differ from more customary approaches in that it incorporates intrinsic noise levels nonlinearly and make explicit the interaction between the mean activity and its correlations. We analyze the dynamics of these equations, with a particular focus on the influence of noise levels on shaping the collective response of neural assemblies and brain states. Cascades of Hopf bifurcations are observed as a function of noise amplitude, for noise levels small enough, and delays, in a finite-population system. The presence of spatially homogeneous solutions in law is discussed in different non-delayed neural fields and an instability, as noise amplitude is varied, of the homogeneous state, is found. In these regimes, very complex irregular and structured spatio-temporal patterns of activity are exhibited including in particular wave or bump splitting.

Keywords: mean-field equations, neural fields, bifurcations, integro-differential equations, noise, infinite-dimensional dynamical systems, propagation of chaos, delayed stochastic integro-differential equations.

Contents

1 Introduction

2

Email address: `jonathan.touboul@college-de-france.fr` (Jonathan Touboul)

2	Mathematical results on mean-fields models for neural fields	4
2.1	Finite number of populations	4
2.2	Infinite number of populations	6
3	Mean-field equations for firing-rate models	12
3.1	Finite-population Wilson and Cowan Equations	13
3.2	Spatially extended neural fields	16
4	Analysis of the solutions	21
4.1	Finite-populations networks	21
4.2	Neural Fields Dynamics	25
4.2.1	A single layer neural field: Turing-Hopf instabilities and noise	26
4.2.2	Dynamic Turing patterns in a two layers neural field with periodic boundary conditions	30
5	Discussion	40
Appendix A Existence and Uniqueness of solutions of the synchronized mean-field solution		43
Appendix B Spatio-temporal patterns for one-dimensional neural fields with reflective or zero boundary conditions		45
Appendix B.1	Reflective boundary conditions	45
Appendix B.2	Zero boundary conditions	45

1. Introduction

The activity of the brain is often characterized by large-scale macroscopic states resulting of the structured interaction of a very large number of neurons. This interaction yield meaningful signals accessible from non-invasive imaging techniques (EEG/MEG) and often used for diagnosis. Finer analysis of the brain's constitution identifies anatomical structures, such as the cortical columns, composed of the order of few thousands to one hundred thousand neurons belonging to a few different species, in charge of specific functions, sharing the same input and strongly interconnected, communicating through the emission of action potentials after delays depending on the anatomical or functional distance between themselves. Two interesting well-understood cortical areas are the primary visual cortex of certain mammals and the rat's barrel cortex. In the primary visual cortex V1, neurons can be divided into orientation preference columns responding to specific orientations in visual stimuli, forming specific patchy connections [1, 2]. Similarly, the rat's barrel cortex presents a clear columnar organization, and neurons responding to the sensory information of a particular whisker anatomically gather into barrels [3, 4]. More generally, it is now understood that brain's activity results from the interactions of different cells, among which neurons, manifesting highly complex behaviors often characterized by the intense presence of noise. The communication between two such columns is characterized by a delay due to the transport of information through axons at a finite speed and to the typical time the synaptic transmission takes. These delays have a clear role in shaping the neuronal activity, as established by different authors (see e.g. [5, 6, 7, 8]). Several relevant brain states rely on the coordinated behaviors of large neural assemblies, and recently raised the interest of

physiologists and computational neuroscientists, among which we shall cite the rapid complex answers to specific stimuli [9], decorrelated activity [10, 11], large scale oscillations [12], synchronization [13, 14], and spatio-temporal pattern formation [15, 16, 17].

Most computational models of neural area have relied on continuum limits ever since the seminal work of Wilson, Cowan and Amari [18, 19, 20, 21], in which the activity is represented through a macroscopic variable, the population-averaged firing rate, that is generally assumed to be deterministic. This approach successfully accounted for several phenomena, for instance for the problem of spatio-temporal pattern formation in spatially extended models (see e.g. [16, 22, 23, 24]). In this approach, the effect of noise is neglected in large populations. Increasingly many models now consider that the different intrinsic or extrinsic noise sources are a meaningful part of the neuronal signal rather than a pure disturbing effect, that conveys important information [25]. For instance, sparsely connected neural networks were studied, in which the sparse connectivity assumption allows studying regimes where the activity is uncorrelated [26, 27, 28]. Again, the emergent global activity of the population in the limit of an infinite number of neurons is deterministic, and evolves according to a mean-field firing rate equation. The stochastic nature of the firing was also developed through such methods as the population density [29], or from a Markovian model governing the firing dynamics of the neurons in the network, where the transition probability satisfies master equation. This modeling recently gathered the interest of the community (see e.g. [30, 31, 32, 33, 34, 35]). Most of these approaches are proved correct in some parameter regions using statistical physics tools such as path integrals and Van-Kampen expansions, and involve a moment expansion and truncation.

We are interested here to start include noise at the level of each individual neuron. From the mathematical viewpoint, each neuron is a diffusion process, and different neurons belong to particular populations in which they receive a common input and are interconnected in a similar fashion. These equations motivated by biological analysis, are studied in a probabilistic setting in a recent paper [36], taking into account spatial information and delayed interconnections, using probabilistic methods from the propagation of chaos domain (see e.g. [37]). The results of this analysis are summarized in section 2. Under mild assumptions on the neuronal dynamics, the regularity of the interactions and the number of neurons per population, this analysis provides a mean-field equation corresponding to the behavior of a particular neuron in the network. These equations, in the original general framework, apply to such neurons as the Hodgkin-Huxley and Fitzhugh-Nagumo neuron models, which are relevant representations of individual neuronal activity. We analyze here the implications of this result in that general setting in the discussion section. We also discuss an extended notion of synchronization, the *synchronization in law*, and provide general conditions for this property to occur in spatially extended mean-field neural fields systems. The mean-field equations obtained in [36] are implicit equations on probability distributions, and as such extremely hard to tame in general. Simulations of such equations are relatively hard to perform, as illustrated in the case where no delay and no spatial extension is taken into account [38], and this difficulty makes it hard to identify qualitative effects of noise levels in such systems. In order to start uncovering the structure of the solutions of these equations and possible effects of noise levels each individual neuron is submitted to, we consider in section 3 a simplified neuron model based on the description of firing-rates. In this particular case, we demonstrate that the solution of the complicated mean-field equations are Gaussian, similarly to what was done in a way simpler model in [39]. Characterizing the mean and covariance functions are hence sufficient to describe the dynamics of the solu-

tions, and these are shown to exactly reduce to a set of deterministic delayed differential or integro-differential equations. The derivation of these equations and the bifurcations of these equations are studied, in the finite-population case (section 3.1) and an intricate bifurcation structure with the appearance of a cascade of Hopf bifurcations as a function of noise levels and delays, that tend to accumulate as delays are increased in a restricted region of noise levels. This bifurcation structure results in the presence of an increasing number of unstable cycles that provoke extremely complex and irregular transient behaviors. In the continuous-populations case (section 3.2), we show noise levels very strongly shape the form of the spatio-temporal solutions of the system. Spatially homogeneous stationary or periodic solutions are found as a function of the noise levels. An additional state is exhibited for small values of the noise levels, in which spatially inhomogeneous, non-stationary spatio-temporal patterns with a complicated shape arise. These qualitative results are reproduced for different unidimensional neural fields with different topologies and connectivities, and either satisfying or not the synchronization in law condition, in appendix [Appendix B](#). Implications of these results are eventually discussed in section 5 together with some open problems the present study motivates.

2. Mathematical results on mean-fields models for neural fields

In [\[36\]](#) a rigorous derivation of the mean-field equations is performed for a wide class of models encompassing classical neuron models such as the Hodgkin-Huxley or the Fitzhugh-Nagumo models, taking into account neural fields spatial structures and space-dependent delays. The general results obtained in that article are summarized here. In all the manuscript, we are working in a complete probability space $(\Omega, \mathcal{F}, \mathbb{P})$ satisfying the usual conditions, and endowed with a filtration $(\mathcal{F}_t)_t$. The *state* of each neuron i in the network is described by a d -dimensional variable $X^i \in E \stackrel{\text{def}}{=} \mathbb{R}^d$, typically corresponding to the membrane potential of the neuron and possibly additional variables such as those related to ionic concentrations and channels. We distinguish the cases where the number of populations is finite and the case where it is infinite corresponding to the spatially extended neural fields.

2.1. Finite number of populations

We start by summarizing the results of [\[36\]](#) in the case where the network is composed of a finite number of populations $\alpha \in \{1, \dots, P\}$. Let p denote the population function that associates to a neuron i the population α it belongs to: $p(i) = \alpha$, and $N_\alpha(N)$ the number of neuron in population α for a network size N (we will generally drop the dependence of N_α in N since no confusion is possible), and assume that this size tends to infinity in the limit $N \rightarrow \infty$. The state of a neuron i in population α , X^i is characterized by its intrinsic dynamics governed by a drift function $G_\alpha : \mathbb{R} \times E \mapsto E$ (including the intrinsic dynamics and the deterministic inputs) and a diffusion matrix $g_\alpha : \mathbb{R} \times E \mapsto \mathbb{R}^m$.

$$dX_t^i = G_\alpha(t, X_t^i) dt + g_\alpha(t, X_t^i) dW_t^i,$$

where $(W_t^i)_{i \in \mathbb{N}}$ constitutes a sequence of $m \times d$ -dimensional adapted Brownian motions. Neuron j of population γ produces an infinitesimal current received at time t by the neuron i modeled as:

$$\frac{1}{N_\gamma} \int_{-\tau}^0 b_{\alpha\gamma}(X_t^i, X_{t+s}^j) d\eta_{\alpha\gamma}(s) dt + \frac{1}{N_\gamma} \int_{-\tau}^0 \beta_{\alpha\gamma}(X_t^i, X_{t+s}^j) d\mu_{\alpha\gamma}(s) dB_t^{i\gamma}.$$

The terms $\eta_{\alpha\gamma}$ and $\mu_{\alpha\gamma}$ denote signed finite measures modeling the delays occurring in the information transmission through the axons, $b_{\alpha\gamma}$ and $\beta_{\alpha\gamma}$ are smooth functions of $E \times E \mapsto E$ and $(B_t^{i,\gamma})_{i \in \mathbb{N}, \gamma=1, \dots, P}$ are $d \times d$ independent adapted Brownian motions. In this setting, the network equations read:

$$\begin{aligned} dX_t^{i,N} = & G_\alpha(t, X_t^{i,N}) dt + \sum_{\gamma=1}^P \sum_{j=1, p(j)=\gamma}^N \frac{1}{N_\gamma} \int_{-\tau}^0 b_{\alpha\gamma}(X_t^{i,N}, X_{t+s}^{j,N}) d\eta_{\alpha\gamma}(s) dt \\ & + g_\alpha(t, X_t^{i,N}) \cdot dW_t^i + \sum_{\gamma=1}^P \frac{1}{N_\gamma} \sum_{j=1, p(j)=\gamma}^N \int_{-\tau}^0 \beta_{\alpha\gamma}(X_t^{i,N}, X_{t+s}^{j,N}) d\mu_{\alpha\gamma}(s) \cdot dB_t^{i\gamma}. \quad (1) \end{aligned}$$

For the sake of simplicity, we will denote in the sequel the sum over neurons of population γ , $\sum_{j=1, p(j)=\gamma}^N$, simply by $\sum_{j=1}^{N_\gamma}$. These equations are well-posed stochastic differential equations on the infinite-dimensional space $\mathcal{C}_\tau = C([- \tau, 0], E)$ (see e.g. [40, 41]) of continuous functions of $[- \tau, 0]$ with values in E . We will generally make the assumption that the network has chaotic initial condition, i.e. independent initial conditions, identically distributed for neurons belonging to the same population. In details, for $(\zeta_0^\alpha(t), \alpha = 1 \dots P) \in \mathcal{C}_\tau$ a stochastic process with independent components, a chaotic initial condition on the network consists in setting the initial condition of all neurons i of population α to an independent copy of ζ_0^α . The following mild technical assumptions on the functions governing the network's dynamics:

- (H1). G_α and g_α are uniformly locally Lipschitz-continuous with respect to their second variable
- (H2). $b_{\alpha\gamma}$ and $\beta_{\alpha\gamma}$ are L -Lipschitz-continuous, i.e. there exists a positive constant L such that for all (x, y) and (x', y') in $E \times E$ we have:

$$|\Theta_{\alpha\gamma}(x, y) - \Theta_{\alpha\gamma}(x', y')| \leq L(|x - x'| + |y - y'|)$$

for $\Theta \in \{b, \beta\}$.

- (H3). There exists a $\tilde{K} > 0$ such that:

$$\max(|b_{\alpha\gamma}(x, z)|^2, |\beta_{\alpha\gamma}(x, z)|^2) \leq \tilde{K}(1 + |x|^2)$$

- (H4). The drift and diffusion functions satisfy the monotone growth condition:

$$x^T f_\alpha(t, x) + \frac{1}{2} |g_\alpha(t, x)|^2 \leq K(1 + |x|^2).$$

Under these assumptions, the following theorem is proved in [36]:

Theorem 1. *Let us consider a network composed of N neurons belonging to P populations. Assuming the regularity assumptions (H1)-(H4) are satisfied and that each neuron of the network chaotic initial conditions (with law $\zeta^{\alpha,0}$ for neurons belonging to the same population α). Fix $l \in \mathbb{N}^*$ and $\{i_1, \dots, i_l\}$ l neurons of the network. The law of $(X_t^{i_1,N}, \dots, X_t^{i_l,N}, -\tau \leq t \leq T)$ solution of the network equations (1) converges towards $m^{p(i_1)} \otimes \dots \otimes m^{p(i_l)}$ when $N \rightarrow \infty$ where m^α is the law of the unique solution \bar{X} of the*

equation:

$$d\bar{X}_t^\alpha = G_\alpha(t, \bar{X}_t^\alpha) dt + \sum_{\gamma=1}^P \int_{-\tau}^0 \mathbb{E}_{\bar{Y}}[b_{\alpha\beta}(\bar{X}_t^\alpha, \bar{Y}_{t+s}^\beta)] d\eta_{\alpha\beta}(s) dt \\ + g_\alpha(t, \bar{X}_t^\alpha) dW_t^\alpha + \sum_{\gamma=1}^P \int_{-\tau}^0 \mathbb{E}_{\bar{Y}}[\beta_{\alpha\beta}(\bar{X}_t^\alpha, \bar{Y}_{t+s}^\beta)] d\mu_{\alpha\beta}(s) dB_t^{\alpha\gamma} \quad (2)$$

with initial condition $(\zeta_t^\alpha, \alpha = 1 \cdots P, t \in [-\tau, 0])$. In equation (2), the process (\bar{Y}_t^γ) is a process independent of \bar{X}_t^γ and has the same law as \bar{X}_t^γ and $\mathbb{E}_{\bar{Y}}$ denotes the expectation with respect to the process \bar{Y} . In other terms, if m_t^γ denotes the probability distribution of \bar{X}_t^γ , the mean-field equations can be equivalently written as:

$$d\bar{X}_t^\alpha = G_\alpha(t, \bar{X}_t^\alpha) dt + \sum_{\gamma=1}^P \int_{-\tau}^0 \int_E b_{\alpha\beta}(\bar{X}_t^\alpha, y) m_{t+s}^\gamma(dy) d\eta_{\alpha\beta}(s) dt \\ + g_\alpha(t, \bar{X}_t^\alpha) dW_t^\alpha + \sum_{\gamma=1}^P \int_{-\tau}^0 \int_E \beta_{\alpha\beta}(\bar{X}_t^\alpha, y) m_{t+s}^\gamma(dy) d\mu_{\alpha\beta}(s) dB_t^{\alpha\gamma}.$$

2.2. Infinite number of populations

We now summarize results of [36] in the case of neural fields spanning over an infinite, continuous compact space Γ , modeling a spatial or functional extension of a cortical structure. These structures are made of several sub-areas, the neural populations, composed of a large number of strongly interconnected neurons. The set Γ considered is a finite-dimensional compact set. Typically, it is considered, when populations are described by their location on the cortex, that Γ as a compact subset of \mathbb{R}^q for some $q \in \mathbb{N}^*$ (in Appendix B, we will consider in particular the case $\Gamma = [0, 1]$). When considering that populations are defined by the neuron's function, the shape of Γ can take different forms depending on the geometry of the feature space. For instance in the case of the modeling of pinwheels primary visual area, neurons are indexed by their preferred orientation that can be represented in the torus $\Gamma = \mathbb{S}^1$ (this is the case of section 4.2).

In that case, the total number of populations is a diverging function $P(N)$ of the total number of neurons N , and populations densely cover Γ in the limit $N \rightarrow \infty$ with a certain density. The populations are characterized by their location $(r_1, \dots, r_{P(N)}) \in \Gamma^{P(N)}$ (see figure Fig. 1), and by the number of neurons in each population in a network of size N , $(N_1(N), \dots, N_{P(N)}(N))$ (we hence have $\sum_{\gamma=1}^{P(N)} N_\gamma(N) = N$). Populations are randomly and independently drawn in a law $\lambda(\cdot)/\lambda(\Gamma)$ where λ is a square integrable¹, finite density over Γ (i.e. a positive function such that $\int_\Gamma \lambda^2(r) dr \stackrel{\text{def}}{=} (\lambda^2)(\Gamma) < \infty$), accounting for possible inhomogeneities of the neural field. Note that the square integrability condition readily implies that $\int_\Gamma \lambda(r) dr \stackrel{\text{def}}{=} \lambda(\Gamma) < \infty$. This degree of freedom allowed for accounting for different topologies and geometries of the physical space or feature space (for instance, a recent model of texture neural field involves a feature space having an hyperbolic geometry,

¹Only integrability was assumed in [36], the square integrability will be needed for our developments on firing-rate models.

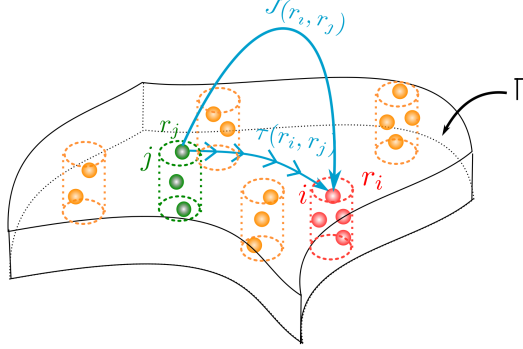


Figure 1: A typical architecture of neural field: cylinders represent neural populations as cortical columns spanning across the cortex. Neuron j in the green population at location $r_j \in \Gamma$ communicates with neuron i in the red population at location r_i , and the information sent is received with a delay $\tau(r_i, r_j)$ depending on the spatial location of each neuron, and with a synaptic weight $J(r_i, r_j)$ also depending on the neural populations of i and j .

see e.g. [42, 43]). The expectation over the realizations of the space locations (r_α) is denoted \mathbb{E} .

As observed in [36], there is a critical competition between the number of populations and the total number of neurons. Indeed, in order for averaging effects to occur in the neural field, a very large number of neurons in each population is required, competing with the number of populations, which is required to fill the space Γ . A technical assumption made in [36] was the following:

$$\mathbb{E}(N) \stackrel{\text{def}}{=} \frac{1}{P(N)} \sum_{\gamma=1}^{P(N)} \frac{1}{N_\gamma(N)} \xrightarrow{N \rightarrow \infty} 0 \quad (3)$$

This assumption ensures heuristically most populations are made of a diverging number of neurons. This interpretation is relevant for our neuronal populations problem since, it is understood that populations roughly contain the same number of neurons and that this number of neurons is orders of magnitude larger than the number of populations (see e.g. [44]). In order to comply with more standard approaches in neural field theory, the functions $G_\alpha(t, x)$ are replaced by $G(r_\alpha, t, x)$ and similarly $g_\alpha(t, x)$ by $g(r_\alpha, t, x)$. The number of populations diverging, it is necessary in our description to scale the synaptic weight as the number of populations increases, in order to ensure the finiteness of the input to one single neuron², and define the interaction functions between population α and population γ at location r_γ , denoted in the finite-population case $b_{\alpha, \gamma}(x, y)$ (resp. $\beta_{\alpha, \gamma}(x, y)$) by $\frac{\lambda(\Gamma)}{P(N)} b(r_\alpha, r_\gamma, x, y)$ (resp. $\frac{\lambda(\Gamma)}{P(N)} \beta(r_\alpha, r_\gamma, x, y)$). The delay measures $\eta(r_\alpha, r_\gamma, s)$ and $\mu(r_\alpha, r_\gamma, s)$ typically involve the distance $\|r_\alpha - r_\gamma\|_\Gamma$ and the transmission velocity of the information in the axons. These are again assumed to be finite signed measures, charging the interval $[-\tau, 0]$, with total variation uniformly (in r_α and r_γ) bounded by a quantity denoted κ .

We define a sequences of independent Brownian motions (W_t^i) in $\mathcal{M}(C([0, T]), \mathbb{R}^{m \times d})$ and

²This is due in particular to the limited resources of the neuronal environment.

a sequence of independent cylindrical Brownian motions $B_t^i(r')$ in $\mathcal{M}(C([0, T]), \mathbb{L}^2(\Gamma, \mathbb{R}^{\delta \times d}))$ for $i \in \mathbb{N}$, i.e. centered Gaussian processes with covariance function $\mathbb{E}[B_t^i(r)B_s^j(r')] = t \wedge s$ if $i = j$ and $r = r'$, and 0 otherwise (see [40] for existence and properties of this process). The stochastic network equations in the read, for $p(i) = \alpha$ and a network of size N :

$$\begin{aligned} dX_t^{i,N} &= G(r_\alpha, t, X_t^{i,N}) dt + \frac{\lambda(\Gamma)}{P(N)} \sum_{\gamma=1}^{P(N)} \sum_{j=1}^{N_\gamma} \frac{1}{N_\gamma} \int_{-\tau}^0 b(r_\alpha, r_\gamma, X_t^{i,N}, X_{t+s}^{j,N}) d\eta(r_\alpha, r_\gamma, s) dt \\ &+ g(r_\alpha, t, X_t^{i,N}) \cdot dW_t^i + \frac{\lambda(\Gamma)}{P(N)} \sum_{\gamma=1}^{P(N)} \sum_{j=1}^{N_\gamma} \frac{1}{N_\gamma} \int_{-\tau}^0 \beta(r_\alpha, r_\gamma, X_t^{i,N}, X_{t+s}^{j,N}) d\mu(r_\alpha, r_\gamma, s) \cdot dB_t^i(r_\gamma). \end{aligned} \quad (4)$$

They make the following suitable regularity assumptions on the functions governing the dynamics of the neurons:

- (GH1). $G(r, t, \cdot)$ and $g(r, t, \cdot)$ are uniformly locally Lipschitz-continuous,
- (GH2). $b(r, r', \cdot, \cdot)$ and $\beta(r, r', \cdot, \cdot)$ are uniformly Lipschitz-continuous, i.e. there exists a positive constant L such that for all (x, y) and (x', y') in $E \times E$ and all $(r, r') \in \Gamma^2$ we have:

$$|\Theta(r, r', x, y) - \Theta(r, r', x', y')| \leq L(|x - x'| + |y - y'|)$$

for $\Theta \in \{b, \beta\}$.

- (GH3). There exists a $\tilde{K} > 0$ such that:

$$\max(|b(r, r', x, z)|^2, |\beta(r, r', x, z)|^2) \leq \tilde{K}(1 + |x|^2)$$

- (GH4). The drift and diffusion functions satisfy, uniformly in space (r) and time (t), the inequality:

$$x^T f(r, t, x) + \frac{1}{2} |g(r, t, x)|^2 \leq K(1 + |x|^2)$$

Under these assumptions, it is proved in [36] the following:

Theorem 2. *Let us consider a network composed of N neurons belonging to $P(N)$ populations such that the assumptions (3), (GH1)-(GH4) are satisfied and that each neuron of the network has independent initial conditions, that are identically distributed population per population (with law $\zeta^0(r)$ for neurons belonging to the population located at $r \in \Gamma$). Fix $l \in \mathbb{N}^*$ and $\{i_1, \dots, i_l\}$ l neurons of the network. The law of $(X_t^{i_1, N}, \dots, X_t^{i_l, N}, -\tau \leq t \leq T)$ solution of the network equations (4) converges towards $m_t(r_{p(i_1)}) \otimes \dots \otimes m_t(r_{p(i_l)})$ when $N \rightarrow \infty$, where $m_t(r)$ is the law of $\bar{X}_t(r)$, the unique solution of the mean-field equations:*

$$\begin{aligned} d\bar{X}_t(r) &= G(r, t, \bar{X}_t(r)) dt + \int_{\Gamma} \int_{-\tau}^0 \mathbb{E}_{\bar{Z}}[b(r, r', \bar{X}_t(r), \bar{Z}_{t+s}(r'))] d\eta(r, r', s) \lambda(r') dr' dt \\ &+ g(r, t, \bar{X}_t(r)) \cdot dW_t(r) + \int_{\Gamma} \int_{-\tau}^0 \mathbb{E}_Z[\beta(r, r', \bar{X}_t(r), \bar{Z}_{t+s}(r'))] d\mu(r, r', s) \cdot dB_t(r, r') \lambda(r') dr' \end{aligned} \quad (5)$$

with initial condition $(\zeta_t^0(r), r \in \Gamma, t \in [-\tau, 0])$, where the process $(Z_t(r))$ is independent of, and has the same law as $\bar{X}_t(r)$.

These results presented in the summary can appear very formal due to the generality of the models considered and to the mathematical approach developed of [36]. However, even at this level of generality, one can deduce several implications of these properties with regards to neuroscience applications (see section 5). It is important to realize at this point that even if the mean-field approach reduces an infinite system of interacting diffusion processes into a single well-posed equation, a major issue one faces is the concrete identification, characterization and simulation of the solution of the mean-field equations. In our spatial and delayed setting, this concern is even more true. We show in this paper that there exists a particular model of neuronal dynamics related to the so-called firing-rate neurons, for which mean-field equations are rigorously reducible to a set of deterministic equations that are amenable to analytic treatment (see sections 3 and 4). We emphasize the fact that firing-rate neurons, though highly popular and widely used in the computational neuroscience community, are not the most relevant from the biological viewpoint, and this restriction justifies the necessity of dealing with such complex models as those described in [36].

A phenomenon of great interest in neuroscience is the synchronization, understood as the fact that neurons manifest the same behavior after a transient phase, or the polychronization corresponding to the fact that the neural field form a few synchronized clusters (see e.g. [14]). Our stochastic setting suggests to extend this notion to the wider notion of *synchronization in law*, corresponding to the fact that the law of state of different neurons or different populations converge (as time increases) towards the same probability distribution. This notion of synchronization generalizes the notion of synchronized oscillations to solutions that are stationary in time, or that present specific time evolutions. In particular, spatially homogeneous in law solutions of the neural field equations will be said synchronized in law. It is clear from the results of theorem 2 that different neurons of the same population in the network have, in the mean-field limit, the same probability distribution provided that they had iid initial conditions, hence synchronize in law, and that different neurons belonging to a few different populations polychronize in law, forming clusters depending on the population the neurons belong to. A more complex question is the synchronization or polychronization in law between different populations. The following proposition provides sufficient conditions for solutions to be spatially homogeneous in law in the neural field setting. To this end, we extend the simple sufficient conditions of [45] in the stochastic mean-field setting. We have the following:

Proposition 3. *Assume that the distribution of the initial condition $\zeta_t^0(r)$ is chaotic and does not depend on $r \in \Gamma$, and that the functions $G(r, t, x)$ and $g(r, t, x)$ does not depend on r . Assume moreover that the law of the quantities:*

$$\begin{cases} B(r, x, \varphi) \stackrel{\text{def}}{=} \int_{\Gamma} \lambda(r') dr' \int_{-\tau}^0 d\eta(r, r', u) b(r, r', x, \varphi(u)) & \text{and} \\ H(r, x, \varphi) \stackrel{\text{def}}{=} \int_{\Gamma} \lambda(r') dr' \int_{-\tau}^0 d\mu(r, r', u) \int_0^t \beta(r, r', x, \varphi(u)) dB_s(r, r') \end{cases} \quad (6)$$

do not depend on r for any φ a measurable function (this ensures that the global input a neuron receives is independent of its spatial location). Then the solution of the mean-field equation (5) is spatially homogeneous (i.e. does not depend on r , or is fully synchronized). Moreover, if we fix $r_0 \in \Gamma$, then for each $r \in \Gamma$, the law of $X_t(r)$ solution of the mean-field

equations is equal to the law of the solution of the equation:

$$\begin{aligned} X_t(r_0) = X_0(r_0) + \int_0^t ds \Big(G(r_0, s, X_s(r_0)) + \mathbb{E}_Z[B(r_0, X_s(r_0), Z_{(\cdot)}(r_0))] \Big) \\ + \mathbb{E}_Z[H(r_0, X_s(r_0), Z_{(\cdot)}(r_0))] + \int_0^t dW_s(r)g(r_0, s, X_s(r_0)). \end{aligned} \quad (7)$$

which has a unique solution.

REMARK. Under the spatial homogeneity condition of proposition 3, two neurons belonging to two different populations r and r' are heuristically interchangeable in the limit $N \rightarrow \infty$, and hence the finite-population setting heuristically applies with only one population network, made of neurons with intrinsic dynamics function $G(r_0, s, x)$ and diffusion function $g(r_0, s, x)$, deterministic (resp. stochastic) interaction functions $B(r_0, x, Z_{(\cdot)}(r_0))$ (resp. $H(r_0, x, Z_{(\cdot)}(r_0))$).

Proof. The existence and uniqueness property of solutions proved in [36] is based on showing a contraction property on the map Φ acting on $\mathcal{M} \stackrel{\text{def}}{=} \mathcal{M}_1(C([-\tau, T], \mathbb{L}_\lambda^2(\Gamma)))$ the space of laws of stochastic processes taking values in $\mathbb{L}_\lambda^2(\Gamma) \stackrel{\text{def}}{=} \mathbb{L}_\lambda^2(\Gamma, E)$ defined, for any $X \in \mathcal{M}$, by:

$$\Phi(X)_t(r) = \begin{cases} \zeta_0^0(r) + \int_0^t ds \left(G(r, s, X_s(r)) + \int_\Gamma \lambda(r') dr' \int_{-\tau}^0 d\eta(r, r', u) \mathbb{E}_Z[b(r, r', X_s(r), Z_{s+u}(r'))] \right) \\ \quad + \int_\Gamma \lambda(r') dr' \int_{-\tau}^0 d\mu(r, r', u) \int_0^t \mathbb{E}_Z[\beta(r, r', X_s(r), Z_{s+u}(r'))] \cdot dB_s(r, r') \\ \quad + \int_0^t dW_s(r)g(r, s, X_s(r)) \quad , \quad t > 0 \\ \zeta_t^0(r) \quad , \quad t \in [-\tau, 0] \\ (Z_t) \stackrel{\mathcal{L}}{=} (X_t) \in \mathcal{M} \text{ independent of } (X_t), (W_t(\cdot)) \text{ and } (B_t(\cdot, \cdot)) \end{cases}$$

It can be shown that the unique solution of the mean-field equations is the limit of the recursion $X_t^{n+1}(r) = \Phi(X_t^n(r))$ starting from any initial process $X_t^0(r)$. Let $X_t^0(r)$ a stochastic process whose law does not depend on r : $X_t^0(r) \stackrel{\mathcal{L}}{=} X_t^0(r_0)$ for any $(r, r_0) \in \Gamma$. We can then

show that $\Phi(X^0)_t(r)$ do not depend on r either, since we have:

$$\begin{aligned}
\Phi(X^0)_t(r) &= X_0^0(r) + \int_0^t ds \left(G(r, s, X_s^0(r)) + \int_{\Gamma} \lambda(r') dr' \int_{-\tau}^0 d\eta(r, r', u) \mathbb{E}_{Z^0}[b(r, r', X_s^0(r), Z_{s+u}^0(r'))] \right) \\
&\quad + \int_{\Gamma} \lambda(r') dr' \int_{-\tau}^0 d\mu(r, r', u) \int_0^t \mathbb{E}_{Z^0}[\beta(r, r', X_s^0(r), Z_{s+u}^0(r'))] \cdot dB_s(r, r') + \int_0^t dW_s(r) g(r, s, X_s^0(r)) \\
&\stackrel{\mathcal{L}}{=} X_0^0(r_0) + \int_0^t ds \left(G(r_0, s, X_s^0(r_0)) + \int_{\Gamma} \lambda(r') dr' \int_{-\tau}^0 d\eta(r, r', u) \mathbb{E}_{Z^0}[b(r, r', X_s^0(r_0), Z_{s+u}^0(r_0))] \right) \\
&\quad + \int_{\Gamma} \lambda(r') dr' \int_{-\tau}^0 d\mu(r, r', u) \int_0^t \mathbb{E}_{Z^0}[\beta(r, r', X_s^0(r_0), Z_{s+u}^0(r_0))] \cdot dB_s(r_0, r') + \int_0^t dW_s(r_0) g(r_0, s, X_s^0(r_0)) \\
&= X_0^0(r_0) + \int_0^t ds \left(G(r_0, s, X_s^0(r_0)) + \mathbb{E}_{Z^0}[B(r, X_s^0(r_0), Z_{(\cdot)}^0(r_0))] \right) \\
&\quad + \mathbb{E}_{Z^0}[H(r, X_s^0(r_0), Z_{(\cdot)}^0(r_0))] + \int_0^t dW_s(r_0) g(r_0, s, X_s^0(r_0)) \\
&\stackrel{\mathcal{L}}{=} X_0^0(r_0) + \int_0^t ds \left(G(r_0, s, X_s^0(r_0)) + \mathbb{E}_Z[B(r_0, X_s^0(r_0), Z_{(\cdot)}^0(r_0))] \right) \\
&\quad + \mathbb{E}_{Z^0}[H(r_0, X_s^0(r_0), Z_{(\cdot)}^0(r_0))] + \int_0^t dW_s(r_0) g(r_0, s, X_s^0(r_0)) \\
&= \Phi(X^0)_t(r_0)
\end{aligned}$$

because of the assumption (6). The sequence of processes $X_t^n(r)$ is hence a sequence of processes whose law is independent of r by an immediate recursion, and so is the limit. Hence the unique solution is spatially homogeneous in law. Moreover, a fixed point of Φ , the solution of the mean-field equation satisfies equation (7).

The existence and uniqueness of solutions of equations (7) is more complicated to prove and necessitates different stochastic calculus arguments. It is outlined in [Appendix A](#). \square

A similar sufficient condition can be derived for polychronization in law is more intricate notationally. Sufficient conditions of the type of that of proposition 3 would involve defining a partition of Γ into different clusters and ensuring that the input received by any neuron in a particular cluster from the other clusters only depends on the cluster the neuron belongs to. Conceptually, this does not differ from the full synchronization in law condition, and would correspond to a new partition of the neural field Γ into subpopulations in which neurons are interchangeable. This condition is more delicate to write. Pathwise synchronization of mean-field neural fields, i.e. the actual convergence of the trajectories of the solution of the network equations for two different neurons is more complicated to ensure in our mean-field setting. Such a property would for instance involve a stochastic contraction property of the mean-field equations that would indeed ensure that the distance between two solutions starting from different initial conditions decreases towards zero. Such properties are not addressed here.

The present section summarized a few theoretical results and gave a formal condition for spatially homogeneous solutions to exist. This very formal approach is now used to investigate a simple neural field model that is amenable to analytic treatment, firing-rates neuron models. We start by theoretically deriving the reduced equations in section 3 before turning our attention to their dynamics in section 4.

3. Mean-field equations for firing-rate models

We revisit, from our probabilist point of view, the seminal works of Wilson and Cowan for finite-populations networks [20] and neuronal tissue [21], and the neural fields with propagation delays [46]. In the work of Wilson and Cowan, the authors emphasized the importance of the presence of delays in the dynamics, a feature which has long been overlooked in the neuroscience community, but that has recently proved essential to shape cortical activity [5, 7, 47]. In that model, the state of each neuron is described by a scalar quantity representing the voltage of each neuron, assumed to have a linear intrinsic dynamics $G_\alpha(t, x) = -x/\theta_\alpha + I_\alpha(t)$ (respectively $G(r, t, x) = -x/\theta(r) + I(r, t)$ in the spatially extended case), that interact through their mean firing rate which is given by a sigmoidal transform of the voltage variable. The delayed interactions are written as a sum over all neurons of a synaptic coefficient only depending on the populations the interacting neurons belong to and a sigmoidal transform of the pre-synaptic neuron (the one sending a current), $b_{\alpha\gamma}(x, y) = J_{\alpha\gamma}S_\gamma(y)$ (resp. $b(r, r', x, y) = J(r, r')S(r', y)$). The functions $S_\gamma(x)$ and $S(r, x)$ are assumed uniformly bounded and uniformly Lipschitz-continuous with respect to x . We enrich the model by taking into account intrinsic noise, i.e. that each neurons integrates a stochastic current driven by a Brownian motion, with a diffusion coefficient $g_\alpha(t, x) = \lambda_\alpha(t)$ (resp. $g(r, t) = \lambda(r, t)$). We also consider that the interconnection weights are noisy, as done in section 2, and specify the function $\beta_{\alpha\gamma}(x, y) = \sigma_{\alpha\gamma}S_\gamma(y)$ (resp. $\beta(r, r', x, y) = \sigma(r, r')S(r', y)$). These models clearly satisfy the assumptions of theorems 1 and 2, and we use these to derive a stochastic version of their equations as the number of neurons tends to infinity. In order to simplify further our analysis, we will assume that the delay measures $\eta_{\alpha\gamma}(u)$ and $\mu_{\alpha,\gamma}(u)$ (respectively $\eta(r, r', u)$ and $\mu(r, r', u)$) are Dirac measures at fixed times $\tau_{\alpha\gamma}$ (respectively at $\tau(r, r')$, which generally can be considered to be $\|r - r'\|_\Gamma/c$ where c would be the transport velocity in the axons).

The equation of the dynamics of neuron i of population α in the network with N neurons reads, in the case of a finite number of populations,

$$dV^{i,N}(t) = \left(-\frac{1}{\theta_\alpha} V^{i,N}(t) + I_\alpha(t) + \sum_{\gamma=1}^P J_{\alpha\gamma} \frac{1}{N_\gamma} \sum_{j=1}^{N_\gamma} S_\gamma(V^{j,N}(t - \tau_{\alpha\gamma})) \right) dt + \lambda_\alpha(t) dW_t^i + \sum_{\gamma=1}^P \sigma_{\alpha\gamma} \left(\frac{1}{N_\gamma} \sum_{j=1}^{N_\gamma} S_\gamma(V^{j,N}(t - \tau_{\alpha\gamma})) \right) dB_t^{i\gamma} \quad (8)$$

and in the case of spatially extended networks:

$$dV^{i,N}(t) = \left(-\frac{1}{\theta(r_\alpha)} V^{i,N}(t) + I(r_\alpha, t) + \sum_{\gamma=1}^{P(N)} J(r_\alpha, r_\gamma) \frac{1}{N_\gamma} \sum_{j=1}^{N_\gamma} S(r_\gamma, V^{j,N}(t - \tau(r_\alpha, r_\gamma))) \right) dt + \Lambda(r_\alpha, t) dW_t^i + \sum_{\gamma=1}^{P(N)} \sigma(r_\alpha, r_\gamma) \left(\frac{1}{N_\gamma} \sum_{j=1}^{N_\gamma} S(r_\gamma, V^{j,N}(t - \tau(r_\alpha, r_\gamma))) \right) dB_t^i(r_\gamma). \quad (9)$$

Note that we will also consider neural fields composed of different layers (for instance excitatory and inhibitory neurons). The above theoretical analysis will readily extend to that case.

In these models, θ_α (resp. $\theta(r_\alpha)$) are the characteristic time of return to rest of neurons in population α if it is not submitted to any input, and these times are assumed to be lowerbounded by a strictly positive value θ_m . The current $I_\alpha(t)$ (resp. $I(r_\alpha, t)$) corresponds to a deterministic input current fed to the neuron, $J_{\alpha\gamma}$ (resp. $J(r_\alpha, r_\gamma)$) is the synaptic weight of the incoming connections from neurons of population γ to neurons of population α and $\sigma_{\alpha\gamma}$ (resp. $\sigma(r_\alpha, r_\gamma)$) its standard deviation, $\lambda_\alpha(t)$ (resp. $\Lambda(r_\alpha, t)$) the standard deviation of the external noise, and the functions $S_\gamma(\cdot)$ (resp. $S(r_\gamma, \cdot)$) are smooth sigmoidal transforms, assumed bounded with bounded derivative.

3.1. Finite-population Wilson and Cowan Equations

As an application of theorem 2, we have:

Proposition 4. *Let $T > 0$ a fixed time. Assume that the initial condition on the network are chaotic, i.e. independent and identically distributed for neurons in the same population. The the state $V^{i,N}$ of neuron in population α , solution of equation (8), converges in law as N goes to infinity towards the process \bar{V}_α unique solution of the mean-field equation:*

$$d\bar{V}_\alpha(t) = \left[-\frac{1}{\theta_\alpha} \bar{V}_\alpha(t) + I_\alpha(t) + \sum_{\beta=1}^P J_{\alpha\beta} \mathbb{E}[S_\beta(\bar{V}_\beta(t - \tau_{\alpha\beta}))] \right] dt + \lambda_\alpha(t) dW_t^\alpha + \sum_{\beta=1}^P \sigma_{\alpha\beta} \mathbb{E}[S_\beta(\bar{V}_\beta(t - \tau_{\alpha\beta}))] dB_t^{\alpha\beta} \quad (10)$$

where the processes (W_t^α) and $B_t^{\alpha\gamma}$ for $\alpha, \gamma \in \{1 \dots P\}^2$ are independent standard real Brownian motions, and the propagation of chaos property applies.

Moreover, if $\bar{V}^0 = (\bar{V}_\alpha^0)_{\alpha=1 \dots P} \in \mathcal{M}^2(\mathcal{C}_\tau)$ is a P -dimensional Gaussian process with independent coordinates, the solution of the mean-field equations (10) with initial conditions \bar{V}^0 are Gaussian processes for all time, with mean denoted $\mu(t) = (\mu_\alpha(t))_{\alpha=1 \dots P}$ and variance $v(t) = (v_\alpha(t))_{\alpha=1 \dots P}$. Let $f_\beta(x, y)$ denote the expectation of $S_\beta(U)$ for U a Gaussian random variable of mean x and variance y . We have:

$$\begin{cases} \dot{\mu}_\alpha(t) = -\frac{1}{\theta_\alpha} \mu_\alpha(t) + \sum_{\beta=1}^P J_{\alpha\beta} f_\beta(\mu_\beta(t - \tau_{\alpha\beta}), v_\beta(t - \tau_{\alpha\beta})) + I_\alpha(t) & \alpha = 1 \dots P \\ \dot{v}_\alpha(t) = -\frac{2}{\theta_\alpha} v_\alpha(t) + \sum_{\beta=1}^P \sigma_{\alpha\beta}^2 f_\beta^2(\mu_\beta(t - \tau_{\alpha\beta}), v_\beta(t - \tau_{\alpha\beta})) + \lambda_\alpha^2(t) & \alpha = 1 \dots P \end{cases} \quad (11)$$

with initial condition $\mu_\alpha(t) = \mathbb{E}[\bar{V}_\alpha^0(t)]$ and $v_\alpha(t) = \mathbb{E}[(\bar{V}_\alpha^0(t) - \mu_\alpha(t))^2]$ for $t \in [-\tau, 0]$. In equation (11), the dot denotes the differential with respect to time.

Proof. It is indeed easy to show that the network equations are of the form of equation (1) with smooth parameters that satisfy the assumptions (H1)- (H4). The first part of the proposition is a direct application of theorem 1. The P equations (10), which are P implicit stochastic differential equations, describe the asymptotic behavior of the network. The unique solution of the mean-field equations (10) with initial condition V^0 can be written in

an implicit form as:

$$V_\alpha(t) = e^{-\frac{t}{\theta_\alpha}} V_\alpha^0 + e^{-\frac{t}{\theta_\alpha}} \left(\int_0^t e^{\frac{s}{\theta_\alpha}} (I_\alpha(s) + \sum_{\beta=1}^P J_{\alpha\beta} \mathbb{E}[S_\beta(V_\beta(s - \tau_{\alpha\beta}))]) ds + \sum_{\beta=1}^P \int_0^t e^{\frac{s}{\theta_\alpha}} \sigma_{\alpha\beta} \mathbb{E}[S_\beta(V_\beta(s - \tau_{\alpha\beta}))]) dB_s^{\alpha\beta} + \int_0^t e^{\frac{s}{\theta_\alpha}} \lambda_\alpha(s) dW_s^\alpha \right). \quad (12)$$

It is clear from this formulation that the righthand side is a Gaussian process as the sum of a deterministic function and of a sum of stochastic integrals of deterministic functions with respect to Brownian motions, and hence so is $V_\alpha(t)$ ³. Its distribution is hence characterized by its mean and covariance functions. The term $\mathbb{E}[S_\beta(V_\beta(s - \tau_{\alpha\beta}))]$, because of the Gaussian nature of V_β , only depends on $\mu_\beta(s - \tau_{\alpha\beta})$ and $v_\beta(s - \tau_{\alpha\beta})$, and is denoted by $f_\beta(\mu_\beta(s - \tau_{\alpha\beta}), v_\beta(s - \tau_{\alpha\beta}))$. Taking the expectation of both sides of the equality (12), we obtain the equation satisfied by the mean of the process $\mu_\alpha(t) = \mathbb{E}[V_\alpha(t)]$:

$$\mu_\alpha(t) = e^{-\frac{t}{\theta_\alpha}} \left(\mu_\alpha(0) + \int_0^t e^{\frac{s}{\theta_\alpha}} \left(\sum_{\beta=1}^P J_{\alpha\beta} f_\beta(\mu_\beta(s - \tau_{\alpha\beta}), v_\beta(s - \tau_{\alpha\beta})) + I_\alpha(s) \right) ds \right).$$

Taking the variance of both sides of the equality (12), we obtain the following equation:

$$v_\alpha(t) = e^{-\frac{2t}{\theta_\alpha}} \left(v_\alpha(0) + \int_0^t e^{\frac{2s}{\theta_\alpha}} \left(\sum_{\beta=1}^P \sigma_{\alpha\beta}^2 f_\beta^2(\mu_\beta(s - \tau_{\alpha\beta}), v_\beta(s - \tau_{\alpha\beta})) + \lambda_\alpha^2(s) \right) ds \right).$$

These two formulae are exactly an integral representation of equations (11) which concludes the proof. \square

REMARK.

- The variance by itself does not characterize the law of the process V , it is necessary to describe the covariance matrix function $C_{\alpha\beta}(t_1, t_2)$ for t_1 and t_2 in \mathbb{R}^{+*} . It is easily shown that for $\alpha \neq \beta$, this correlation is null, and moreover:

$$C_{\alpha\alpha}(t_1, t_2) = e^{-\frac{t_1+t_2}{\theta_\alpha}} v_\alpha(0) + \int_0^{t_1 \wedge t_2} e^{\frac{2s}{\theta_\alpha}} \lambda_\alpha(s)^2 ds + \int_0^{t_1 \wedge t_2} e^{\frac{2s}{\theta_\alpha}} \sum_{\beta=1}^P \sigma_{\alpha\beta}^2 f_\beta^2(\mu_\beta(s - \tau_{\alpha\beta}), v_\beta(s - \tau_{\alpha\beta})) ds$$

for $t_1, t_2 \in \mathbb{R}^{+*}$, hence only depends on the parameters of the system and on the functions $\mu_\beta(t)$ and $v_\beta(t)$. The description of the solution given by equations (11) is hence sufficient to fully characterize the solution of the mean-field equations (10).

³This property can also be proved by using the classical characterization of the solution of the mean-field equation as the limit of the iteration of the map Φ as proved in [36]. In that case, similarly to the proof provided in [39] for non-delayed finite-populations equations, \bar{V} is defined the limit of a sequence of Gaussian processes, hence Gaussian itself.

- In the case where the sigmoidal transforms are of the form $S_\alpha(x) = \text{erf}(g_\alpha x + h_\alpha)$, a simple calculation based on a change of variable shows that the functions $f_\alpha(\mu_\alpha, v_\alpha)$ involved in the reduced mean-field equations (11) take the simple form (see [39] for the calculations):

$$f_\alpha(\mu, v) = \text{erf}\left(\frac{g_\alpha \mu + h_\alpha}{\sqrt{1 + g_\alpha^2 v}}\right).$$

This simple expression motivates the choice of erf sigmoidal functions for further developments.

We can hence reduce the complex mean-field equation (10) into the simpler system of coupled delayed differential equations (DDEs) (11), which allows a simple analysis of the solutions and the dependency of the behavior upon the parameters. Even if we know that there exists a unique solution to the mean-field equations, and that necessarily the solution starting from Gaussian chaotic initial condition is Gaussian with mean and standard deviation satisfying equations (11), it is necessary to show that these latter equations are well-posed and that they have a unique solution. Let us denote by \mathcal{C} the Banach space of continuous functions mapping $[-\tau, 0]$ into E^{2P} endowed with the topology of the uniform convergence. Following Hale and Lunel [48], we consider the moment equations (11) as ordinary differential equations on \mathcal{C} . We have the following:

Theorem 5. *Under the assumptions that:*

- $t \mapsto I_\alpha(t)$ and $t \mapsto \lambda_\alpha(t)$ are continuous,
- $\lambda_\alpha(t) \geq \lambda_0 > 0$ for any $t > 0$ and $\alpha \in \{1, \dots, P\}$,
- the sigmoid functions S_γ have bounded derivatives
- The initial conditions on the variance $v_\alpha^0 \in C([-\tau, 0], \mathbb{R})$ satisfies $v_\alpha^0(t) \geq v_0 > 0$ for $t \in [-\tau, 0]$ and $\alpha \in \{1, \dots, P\}$.

there exists a unique solution to the moment equations (11) starting from an initial condition $\mu_\alpha^0 \in C([-\tau, 0], \mathbb{R})$ and v_α^0 .

Proof. This theorem is a simple application of theorems [48, Thm 2.1 and 2.3]. These results ensure existence and uniqueness of solutions as soon as the vector field is Lipschitz-continuous in \mathcal{C} and continuous in time. Thanks to uniform lowerbound of the functions λ_α and of the initial condition on the variances v_α^0 , we clearly have $v(t) \geq v_m \stackrel{\text{def}}{=} \min(v_0, \lambda_0^2 \theta_m / 2)$ (we recall that θ_m is the strictly positive lower bound of the characteristic times θ_α). We have:

$$f_\gamma(x, y) = \frac{1}{\sqrt{2\pi y}} \int_{\mathbb{R}} S_\gamma(z) e^{\frac{(z-x)^2}{2y}} = \int_{\mathbb{R}} S_\gamma(z\sqrt{y} + x) \frac{e^{-z^2/2}}{\sqrt{2\pi}} dz.$$

Thanks to the properties of the integral term and in particular the fast convergence towards 0 of the exponential term ensuring existence of moments of any order of the Gaussian, it is straightforward to show that derivative with respect to x and y read:

$$\begin{cases} \frac{\partial f_\gamma(x, y)}{\partial x} &= \int_{\mathbb{R}} S'_\gamma(z\sqrt{y} + x) \frac{e^{-z^2/2}}{\sqrt{2\pi}} dz \\ \frac{\partial f_\gamma(x, y)}{\partial y} &= \int_{\mathbb{R}} z S'_\gamma(z\sqrt{y} + x) \frac{e^{-z^2/2}}{2\sqrt{2\pi y}} dz \end{cases} \quad (13)$$

which are both uniformly bounded on $\mathbb{R} \times [v_m, \infty)$ thanks to the fact that the sigmoids have bounded derivatives and that $y \geq v_0$, since we have:

$$\begin{cases} \left| \frac{\partial f_\gamma(x, y)}{\partial x} \right| & \leq \|S'_\gamma\|_\infty \\ \left| \frac{\partial f_\gamma(x, y)}{\partial y} \right| & \leq \frac{\|S'_\gamma\|_\infty}{2\sqrt{v_0}} \int_{\mathbb{R}} |z| \frac{e^{-z^2/2}}{\sqrt{2\pi}} dz = \frac{\|S'_\gamma\|_\infty}{\sqrt{v_0}} \int_0^\infty z \frac{e^{-z^2/2}}{\sqrt{2\pi}} dz = \frac{\|S'_\gamma\|_\infty}{\sqrt{2\pi v_0}} \end{cases}$$

This property ensures global Lipschitz continuity of the vector field. The differentiability of the vector field with respect to time readily follows from the differentiability of the input and standard deviation functions. We are hence in the application domain of theorems [48, Thm 2.1 and 2.3] and we have existence and uniqueness of solutions for the reduced mean-field equations (11). \square

REMARK. Note that the conditions of theorem 5 are not optimal. For instance in the case $S_\alpha(x) = \text{erf}(g_\alpha x + h_\alpha)$, we already remarked that we had

$$f_\alpha(\mu, v) = \text{erf}\left(\frac{g_\alpha \mu + h_\alpha}{\sqrt{1 + g_\alpha^2 v}}\right)$$

and this function is globally Lipschitz continuous on $\mathbb{R} \times \mathbb{R}^+$, as one can easily check by computing exactly the derivatives of this function with respect to μ and v . The condition on the uniform lowerbound of $\lambda_\alpha(t)$ in theorem 5 can hence be omitted when one chooses erf sigmoidal transforms for instance.

3.2. Spatially extended neural fields

We now consider the infinite-population case of firing-rate neuron models. We assume that we are a priori given a connectivity map with mean $J(r, r')$ and standard deviation $\sigma(r, r')$, a density $\lambda(r)$ such that the neural populations are drawn independently according to this law (after renormalization) as the number of neurons increases. Using theorem 2, we can state the following proposition:

Proposition 6. Let $T > 0$ a fixed time. The process $V^{i, N}$ for i in population α at location $r_\alpha \in \Gamma$, solution of equation (9) with chaotic initial conditions, converges in law towards the process $\bar{V}(r_\alpha)$ where $(\bar{V}_t(r))$ is the unique solution of the mean-field equation:

$$\begin{aligned} d\bar{V}_t(r_\alpha) = & \left[-\frac{1}{\theta(r_\alpha)} \bar{V}_t(r_\alpha) + I(r_\alpha, t) + \int_{\Gamma} \lambda(r') dr' J(r_\alpha, r') \mathbb{E}[S(r', \bar{V}_{t-\tau(r_\alpha, r')}(r'))] \right] dt \\ & + \Lambda(r_\alpha, t) dW_t(r_\alpha) + \int_{\Gamma} \sigma(r_\alpha, r') \mathbb{E}[S(r', \bar{V}_{t-\tau(r_\alpha, r')}(r'))] dB_t(r_\alpha, r') \lambda(r') dr' \end{aligned} \quad (14)$$

where the processes $(W_t(r))$ and $(B_t(r, r'))$ are independent cylindrical Brownian motions, and the propagation of chaos applies.

Moreover, if the initial condition $\bar{V}^0(r) \in \mathcal{M}^2(C([- \tau, 0]), \mathbb{L}_\lambda^2(\Gamma))$ is a cylindrical Gaussian process, the solution of the mean-field equations (10) with initial conditions $\bar{V}^0(r)$ is Gaussian for all time. Denoting by $\mu(r, t)$ its mean, by $v(r, t)$ its variance, and by $f(r, x, y)$ the expectation of $S(r, U)$ for U a Gaussian random variable of mean x and variance y . We

have:

$$\begin{cases} \frac{\partial \mu}{\partial t}(r, t) = -\frac{1}{\theta(r)} \mu(r, t) + \int_{\Gamma} \lambda(r') dr' J(r, r') f(r, \mu(r', t - \tau(r, r')), v(r', t - \tau(r, r'))) + I(r, t) \\ \frac{\partial v}{\partial t}(r, t) = -\frac{2}{\theta(r)} v(r, t) + \int_{\Gamma} \lambda(r')^2 dr' \sigma(r, r')^2 f(r, \mu(r', t - \tau(r, r')), v(r', t - \tau(r, r'))) + \Lambda^2(r, t) \end{cases} \quad (15)$$

with initial condition $\mu(r, t) = \mathbb{E}[\bar{V}_t^0(r)]$ and $v(r, t) = \mathbb{E}[(\bar{V}_t^0(r, t) - \mu(r, t))^2]$ for $t \in [-\tau, 0]$ and $r \in \Gamma$.

Proof. This proof is essentially identical to that of proposition 4. Indeed, it again appears clearly that the network equations are of the form of equation (4) with parameters satisfying the assumption of section 2.2, and hence that theorem 2 applies. The unique solution of the mean-field equations (10) with initial condition V^0 satisfies the implicit equation:

$$\begin{aligned} V(r, t) = & e^{-\frac{t}{\theta(r)}} V_0^0(r) + e^{-\frac{t}{\theta(r)}} \left(\int_0^t e^{\frac{s}{\theta(r)}} (I(r, s) + \int_{\Gamma} \lambda(r') dr' J(r, r') \mathbb{E}[S(r', \bar{V}_{t-\tau(r, r')}(r'))]) ds \right. \\ & \left. + \int_0^t e^{\frac{s}{\theta(r)}} \Lambda(r, s) dW_s(r) + \int_{\Gamma} \sigma(r, r') \int_0^t e^{\frac{s}{\theta(r)}} \mathbb{E}[S(r', \bar{V}_{t-\tau(r, r')}(r'))] dB_s(r, r') \lambda(r') dr' \right). \end{aligned} \quad (16)$$

and is hence necessarily Gaussian since the righthand side obviously is. Its mean, denoted by $\mu(r, t)$, and variance $v(r, t)$, satisfy the equations:

$$\begin{cases} \mu(r, t) = e^{-\frac{t}{\theta(r)}} \left(\mu(r, 0) + \int_0^t e^{\frac{s}{\theta(r)}} \left(I(r, s) + \int_{\Gamma} \lambda(r') dr' J(r, r') f(r', \mu(r', s - \tau(r, r')), v(r', s - \tau(r, r'))) \right) ds \right) \\ v(r, t) = e^{-\frac{2t}{\theta(r)}} \left(v(r, 0) + \int_0^t e^{\frac{2s}{\theta(r)}} \left(\Lambda(r, s)^2 + \int_{\Gamma} \lambda^2(r') dr' \sigma^2(r, r') f^2(r', \mu(r', s - \tau(r, r')), v(r', s - \tau(r, r'))) \right) ds \right), \end{cases}$$

which concludes the proof. \square

REMARK. Here again, mean and variance are enough to define the law of the stochastic process, since the covariance matrix between $\bar{V}(r, t_1)$ and $\bar{V}(r', t_2)$, $C(r, r', t_1, t_2)$ for t_1 and t_2 in \mathbb{R}^{+*} and $(r, r') \in \Gamma$ only depends on these two quantities. Indeed, for $r \neq r'$, the covariance is null because of the cylindrical nature of the Brownian motions involved and of the initial conditions. It is easily shown that for $r = r'$:

$$\begin{aligned} C(r, r, t_1, t_2) = & e^{-\left(\frac{t_1+t_2}{\theta(r)}\right)} v^\alpha(0) + \int_0^{t_1 \wedge t_2} e^{\frac{2s}{\theta(r)}} \Lambda(r, s)^2 ds \\ & + \int_0^{t_1 \wedge t_2} e^{\frac{2s}{\theta(r)}} \int_{\Gamma} \lambda(r')^2 dr' \sigma(r, r')^2 f^2(r', \mu(r', s - \tau(r, r')), v(r', s - \tau(r, r'))) ds \end{aligned}$$

The description of the solution given by equations (15) is hence sufficient to fully characterize the solution of the mean-field equations (14).

We therefore describe in this formalism the stochastic dynamics of a neural field through two coupled integro-differential equations, instead of just one in the classical cases: the standard deviation of the process is now incorporated to the dynamics of the mean activity, and in the non-noisy case, correspond exactly to more classical neural field equations [46, 49, 50].

Similarly to what was done in the finite-population case, it remains to show that reduced system on the moments (14) is well-posed, to ensure that these equations uniquely characterize the mean-field equations. This is the case under the following conditions:

Theorem 7. *For the sake of simplicity, we assume here that the density function $\lambda(r)$ is upperbounded by a constant A . Under the assumptions that:*

- J is square integrable with respect to Lebesgue's measure on Γ^2 , i.e. belongs to $\mathbb{L}^2(\Gamma^2, \mathbb{R})$,
- σ^2 is square integrable with respect to Lebesgue's measure on Γ^2 ,
- the external current $I(r, t)$ is a bounded, continuous functions of time taking values in $\mathbb{L}^2(\Gamma, \mathbb{R})$
- the external noise $\Lambda^2(r, t)$ is a continuous functions of time taking values in $\mathbb{L}^2(\Gamma, \mathbb{R})$, and is uniformly lowerbounded by a strictly positive constant: $\Lambda(r, t)^2 \geq \Lambda_0^2 > 0$ for all $(r, t) \in \Gamma \times \mathbb{R}^+$,
- The derivative of $S(r, x)$ with respect to its second variable is uniformly bounded,

then for any initial condition $\mu(r, t) \in C([-\tau, 0], \mathbb{L}^2(\Gamma, \mathbb{R}))$ and $v(r, t) \in C([-\tau, 0], \mathbb{L}^2(\Gamma))$ uniformly lowerbounded by a quantity $v_0 > 0$, there exists a unique solution to the moments mean-field equations (14) which moreover belongs to $C([-\tau, T], L^2(\Gamma, \mathbb{R}^2))$.

Proof. The moment mean-field equations (14) constitute a dynamical system in the Banach spaces of functions of Γ with values in \mathbb{R}^2 . It is well known that the space of functions in $\mathcal{B} \stackrel{\text{def}}{=} C([-\tau, T], L^2(\Gamma, \mathbb{R}^2))$ endowed with the norm:

$$\|(\varphi_1, \varphi_2)\|_{\mathcal{B}} = \sup_{s \in [-\tau, T]} \left(\int_{\Gamma} |\varphi_1(r, s)|^2 dr + \int_{\Gamma} |\varphi_2(r, s)|^2 dr \right)^{1/2}$$

is a Banach space. We will show the existence and uniqueness of solutions in this space. We further define the norm up to time $t > 0$ of two elements of \mathcal{B} by:

$$D_t(\varphi_1, \varphi_2) = \sup_{s \in [-\tau, t]} \left(\int_{\Gamma} |\varphi_1(r, s)|^2 dr + \int_{\Gamma} |\varphi_2(r, s)|^2 dr \right).$$

Let us start by ensuring that any possible solution is bounded in this space. We recall that:

$$\begin{aligned} \mu(r, t) = e^{-\frac{t}{\theta(r)}} & \left(\mathbb{E} [V_0^0(r)] + \int_0^t e^{\frac{s}{\theta(r)}} \left(I(r, s) \right. \right. \\ & \left. \left. + \int_{\Gamma} \lambda(r') dr' J(r, r') f(r', \mu(r', s - \tau(r, r')), v(r', s - \tau(r, r'))) \right) ds \right) \end{aligned}$$

and hence we have:

$$\begin{aligned}
\|\mu(\cdot, t)\|_{\mathbb{L}^2(\Gamma, \mathbb{R})}^2 &\leq 3 \left(\|\mathbb{E}[V_0^0(\cdot)]\|_{\mathbb{L}^2(\Gamma, \mathbb{R})}^2 + \int_{\Gamma} dr \left| \int_0^t I(r, s) ds \right|^2 \right. \\
&\quad \left. + \int_{\Gamma} dr \left| \int_0^t ds \int_{\Gamma} \lambda(r') dr' J(r, r') f(r', \mu(r', s - \tau(r, r')), v(r', s - \tau(r, r'))) \right|^2 \right) \\
&\leq 3 \left(\|\mathbb{E}[V_0^0(\cdot)]\|_{\mathbb{L}^2(\Gamma, \mathbb{R})}^2 + T^2 \sup_{t \in [0, T]} \|I(\cdot, s)\|_{\mathbb{L}^2(\Gamma, \mathbb{R})}^2 \right. \\
&\quad \left. + T \lambda(\Gamma) \int_{\Gamma} dr \int_0^t ds \int_{\Gamma} \lambda(r') dr' |J(r, r')|^2 \|f\|_{\infty}^2 \right) \\
&\leq 3 \left(\|\mathbb{E}[V_0^0(\cdot)]\|_{\mathbb{L}^2(\Gamma, \mathbb{R})}^2 + T^2 \sup_{t \in [0, T]} \|I(\cdot, s)\|_{\mathbb{L}^2(\Gamma, \mathbb{R})}^2 + T^2 A \lambda(\Gamma) \|J(r, r')\|_{\mathbb{L}^2(\Gamma^2, \mathbb{R})}^2 \|f\|_{\infty}^2 \right)
\end{aligned}$$

where $\|f\|_{\infty}$ is the uniform upperbound of $f(r, \mu, v)$ in \mathbb{R} , which is smaller or equal to the uniform supremum of the function $x \mapsto S(r, x)$ (which exists by assumption). The same types of calculations allow proving that:

$$\|v(\cdot, t)\|_{\mathbb{L}^2(\Gamma, \mathbb{R})}^2 \leq 3 \left(\|v(\cdot, 0)\|_{\mathbb{L}^2(\Gamma, \mathbb{R})}^2 + T^2 \sup_{t \in [0, T]} \|\Lambda^2(\cdot, s)\|_{\mathbb{L}^2(\Gamma, \mathbb{R})}^2 + T^2 (\lambda^2)(\Gamma) A^2 \|\sigma^2(r, r')\|_{\mathbb{L}^2(\Gamma^2, \mathbb{R})}^2 \|f\|_{\infty}^4 \right).$$

These bounds do not depend upon time t and hence prove that any solution of the moment mean-field equations have bounded norms in the space \mathcal{B} .

Routine methods for this type of infinite-dimensional systems ensure existence and uniqueness of solutions as soon as the vector field of the equation is Lipschitz-continuous for this norm. In our case, similarly to what was done in the proof of theorem 5, it is easy to show under the assumptions of the theorem that the standard deviation $v(r, t)$ is uniformly lowerbounded by a minimal strictly positive value $v_m = \min(v_0, \Lambda_0^2 \theta_m / 2)$, and hence ensuring the global uniform in r Lipschitz-continuity of the function $(\mu, v) \mapsto f(r, \mu, v)$. Let us define for $(\mu, v) \in \mathcal{B}$ the transformation $\Phi(\mu, v)$ taking values in \mathcal{B} and defined by:

$$\left(\begin{array}{l} e^{-\frac{t}{\theta(r)}} \left(\mu(0, r) + \int_0^t e^{\frac{s}{\theta(r)}} \left(I(r, s) + \int_{\Gamma} \lambda(r') dr' J(r, r') f(r', \mu(r', s - \tau(r, r')), v(r', s - \tau(r, r'))) \right) ds \right) \\ e^{-\frac{2t}{\theta(r)}} \left(v(0, r) + \int_0^t e^{\frac{2s}{\theta(r)}} \left(\Lambda^2(r, s) + \int_{\Gamma} \lambda(r')^2 dr' \sigma^2(r, r') f^2(r', \mu(r', s - \tau(r, r')), v(r', s - \tau(r, r'))) \right) ds \right) \end{array} \right)$$

It is clear that any solution of the moment equations are fixed points of Φ and reciprocally. Since $(\mathcal{B}, \|\cdot\|_{\mathcal{B}})$ is a Banach space, showing existence and uniqueness of solutions, i.e. of fixed points of Φ , amounts showing a contraction property on Φ . First of all, similarly to what was done to show that any solutions of the moment equations were bounded in \mathcal{B} , it is very easy to show that for any $(\mu, v) \in \mathcal{B}$, we have $\Phi(\mu, v) \in \mathcal{B}$. We use the classical iteration method to show existence and uniqueness of fixed point. To this end, we fix $\varphi^0 = (\mu^0, v^0) \in \mathcal{B}$ arbitrarily and define the sequence $\varphi^n = (\mu^n, v^n)_{n \in \mathbb{N}}$ iteratively by setting $(\mu^{n+1}, v^{n+1}) = \Phi(\mu^n, v^n)$. We recall that f is Lipschitz-continuous as shown in the proof of theorem 5, and we denote by L the uniform Lipschitz constant of $f(r, x, y)$ in its two last variables. The function $f^2(r, x, y)$ is hence also uniformly Lipschitz-continuous in its two last variables with the Lipschitz constant $2\|f\|_{\infty}L$. Let us now show that the vector

field Φ is Lipschitz-continuous on \mathcal{B} . Let us fix $\varphi_1 = (\mu_1, v_1)$ and $\varphi_2 = (\mu_2, v_2)$ two elements of \mathcal{B} . We have:

$$\begin{aligned} D_t(\varphi_1, \varphi_2) = & \sup_{s \in [-\tau, t]} \left\{ \int_{\Gamma} dr \left| \int_0^t \int_{\Gamma} \lambda(r') dr' J(r, r') \left(f(r', \mu_1(r', s - \tau(r, r')), v_1(r', s - \tau(r, r'))) \right. \right. \right. \\ & \left. \left. \left. - f(r', \mu_2(r', s - \tau(r, r')), v_2(r', s - \tau(r, r'))) \right) ds \right|^2 \right. \\ & \left. + \int_{\Gamma} dr \left| \int_0^t \int_{\Gamma} \lambda^2(r') dr' \sigma^2(r, r') \left(f^2(r', \mu_1(r', s - \tau(r, r')), v_1(r', s - \tau(r, r'))) \right. \right. \right. \\ & \left. \left. \left. - f^2(r', \mu_2(r', s - \tau(r, r')), v_2(r', s - \tau(r, r'))) \right) ds \right|^2 \right\} \end{aligned}$$

The two terms of the righthand side are treated similarly, let us hence deal with the first one. We have:

$$\begin{aligned} & \int_{\Gamma} dr \left| \int_0^t \int_{\Gamma} \lambda(r') dr' J(r, r') \left(f(r', \mu_1(r', s - \tau(r, r')), v_1(r', s - \tau(r, r'))) \right. \right. \\ & \quad \left. \left. - f(r', \mu_2(r', s - \tau(r, r')), v_2(r', s - \tau(r, r'))) \right) ds \right|^2 \\ & \leq T \int_{\Gamma} dr \int_0^t \left| \int_{\Gamma} \lambda(r') dr' J(r, r') \left(f(r', \mu_1(r', s - \tau(r, r')), v_1(r', s - \tau(r, r'))) \right. \right. \\ & \quad \left. \left. - f(r', \mu_2(r', s - \tau(r, r')), v_2(r', s - \tau(r, r'))) \right) ds \right|^2 \\ & \leq T \int_{\Gamma} dr \int_0^t \left(\int_{\Gamma} \lambda(r') dr' J(r, r')^2 \right) \left(\int_{\Gamma} \lambda(r') dr' \left(f(r', \mu_1(r', s - \tau(r, r')), v_1(r', s - \tau(r, r'))) \right. \right. \\ & \quad \left. \left. - f(r', \mu_2(r', s - \tau(r, r')), v_2(r', s - \tau(r, r'))) \right) \right)^2 ds \\ & \leq 2 L^2 T \int_{\Gamma} dr \int_0^t \left(\int_{\Gamma} \lambda(r') dr' J(r, r')^2 \right) \left(\int_{\Gamma} \lambda(r') dr' |\mu_1(r', s - \tau(r, r')) - \mu_2(r', s - \tau(r, r'))|^2 \right. \\ & \quad \left. + |v_1(r', s - \tau(r, r')) - v_2(r', s - \tau(r, r'))|^2 \right) ds \\ & \leq 2 A^2 L^2 T \int_{\Gamma} dr \int_0^t \int_{\Gamma} dr' J(r, r')^2 \|\varphi_1(\cdot, s - \tau(r, r')) - \varphi_2(\cdot, s - \tau(r, r'))\|_{\mathbb{L}^2(\Gamma, \mathbb{R}^2)}^2 \\ & \leq 2 A^2 L^2 T^2 \|J\|_{L^2(\Gamma \times \Gamma)}^2 \int_0^t D_s(\varphi_1, \varphi_2) ds \end{aligned}$$

Similarly, the second term is upperbounded by $8 A^4 L^2 \|f\|_{\infty}^2 T^2 \|\sigma^2\|_{L^2(\Gamma \times \Gamma)}^2 \int_0^t D_s(\varphi_1, \varphi_2) ds$. These two bounds do not depend upon time, hence we have:

$$D_t(\varphi_1, \varphi_2) \leq K' \int_0^t D_s(\varphi_1, \varphi_2) ds$$

with $K' = 2 A^2 L^2 T^2 (\|J\|_{L^2(\Gamma \times \Gamma)}^2 + 4 A^2 \|\sigma^2\|_{L^2(\Gamma \times \Gamma)}^2)$. Routine methods allow showing that:

$$D_t(\varphi^n, \varphi^{n-1}) \leq \frac{(K't)^n}{n!} D_T(\varphi^1, \varphi^0)$$

and hence $\|\varphi^n - \varphi^{n-1}\|_{\mathcal{B}} \leq \sqrt{(K't)^n/n!} \|\varphi^1 - \varphi^0\|_{\mathcal{B}}$, readily implying that φ^n is a Cauchy sequence in the complete space \mathcal{B} and hence converging in \mathcal{B} towards a fixed point of Φ . Uniqueness of the solution is also classically deduced from the above inequality. \square

The well-posedness of the moment equations allows studying the solutions of the stochastic mean-field equations through the analysis of the dynamical system (15).

4. Analysis of the solutions

Now that mean-field equations for firing-rate models were derived, we numerically and analytically analyze their solutions. We investigate separately the effect of delays on the solutions in a finite-population network, and spatially extended neural fields equations with or without delays. The specific effects of propagation delays in neural fields is not analyzed here.

4.1. Finite-populations networks

We analyze in this section the effect of delays in the dynamics of finite-populations neural fields. To fix ideas, we start by a numerical analysis of a simple 2-populations model composed of one excitatory and one inhibitory population, with synaptic weights:

$$J = \begin{pmatrix} 15 & -12 \\ 16 & -5 \end{pmatrix}, \quad (17)$$

and constant delays τ . The time constants θ_1 and θ_2 are set to 1, and the noise on the synaptic connectivity $\sigma_{\alpha\gamma}$ are all null. The currents are fixed to $I_1 = 0$, $I_2 = -3$, and both populations have a common noise intensity λ . The bifurcation diagram of the system (11) as a function of the noise intensity λ and the delay τ is produced in Figure 2. Two branches of fixed points are identified, and as delays are increased, one of the branches of fixed points undergoes a cascade of Hopf bifurcations. The different curves of Hopf bifurcations accumulate on the first curve as delays are increased, on a parameter region where the related fixed point is unstable (see Figure 2(e)). These Hopf are not related to eigenvalues having the largest real part, and hence has no effect on the number or stability of fixed point. These Hopf bifurcations are associated with unstable limit cycles, the accumulation of which produce a complex landscape resulting in very irregular transient behaviors. When fixing a value for the delays to $\tau = 0.5$ (green line of figure 2(a)), we observe in this diagram different ranges of parameter values corresponding to different asymptotic behaviors: stationary solution (blue region), bistability between a stationary and a periodic solution (yellow region), and periodic solutions (orange region, see Fig. 2(e)). The oscillatory region corresponds to a precise synchronization of all neurons (see figure 2(f)), a highly relevant phenomenon in neural systems sometimes related to pathologies such as epilepsy. Fixing $\tau = 5$ corresponds to a case where the system displays seven Hopf bifurcations. The codimension two bifurcation diagram of the system as a function of the input current I_1 and the noise level λ is given in Figure 2(c). We observe that the saddle-node bifurcation forms a cusp, and on one of the branch of the codimension two saddle-node bifurcation curve appears a Bogdanov-Takens and two degenerate Bogdanov-Takens bifurcations. These degenerate bifurcations correspond to the tangential pairing of two Hopf bifurcations merging with the saddle-node manifold. These are non-generic bifurcation but appear structurally stable in these equations. The precise study of the unfolding of these bifurcations is not in the scope

of the present paper, but the unfolding of that bifurcations would be helpful to further understand the local behavior of the system around these singular points. An interesting feature of the system is that delays create complex phenomena only in a restricted region of parameters corresponding to small noise values: for noise large enough, no instability is found, illustrating quantitatively the stabilization effect of the noise. It also illustrates the strong impact of noise in shaping the qualitative form of the solution of the mean-field equations: for small noise, a stationary behavior is found, for intermediate values a periodic orbit is found corresponding to the synchronization of different neurons in the network (see Figure 2(f)) and for larger values of noise, a stationary behavior is again obtained.

The previous example was particularly interesting because noise induced the presence of regular oscillations. However, its particular dynamics and parameters do not allow further mathematical investigation because the characterization of fixed point was not analytically explicit and hence it was hard to characterize the local bifurcations. In order to analytically investigate this kind of system and in particular account for the cascade of Hopf bifurcations numerically exhibited in the previous example, we now simplify the problem by considering a similar neural network model with connectivity matrix:

$$J = \begin{pmatrix} 1 & -1 \\ 1 & 1 \end{pmatrix},$$

and input currents $I_1 = 0$ and $I_2 = -1$. In this case, $\mu_1 = \mu_2 = 0$, $v_1 = v_2 = \lambda^2/2$ is a fixed point of the equation. The characteristic matrix governing the linear stability of this solution reads:

$$A(\zeta) = -(\zeta + 1)Id + \frac{g}{\sqrt{2\pi(1 + g^2\lambda^2/2)}}Je^{-\zeta\tau},$$

whose eigenvalues (the *characteristic roots*) are:

$$\nu_{\pm} = -(\zeta + 1) + \frac{g}{\sqrt{2\pi(1 + g^2\lambda^2/2)}}e^{-\zeta\tau}(1 \pm \mathbf{i})$$

with $\mathbf{i}^2 = -1$, and the *characteristic equation*, defined as $\Delta(\zeta) = \det(A(\zeta))$, vanishes for values of ζ such that at least one of the characteristic roots vanishes, i.e. for ζ such that

$$-(\zeta + 1) + \frac{g}{\sqrt{2\pi(1 + g^2\lambda^2/2)}}e^{-\zeta\tau}(1 \pm \mathbf{i}) = 0 \quad (18)$$

This equation can be solved using the complex branches of Lambert's $(W_k)_{k \in \mathbb{Z}}$ functions (see e.g. [53]). Simple algebra yields the following formula for the characteristic roots of the system:

$$\zeta_{\pm}^k = -1 + \frac{1}{\tau}W_k \left(\frac{g}{\sqrt{2\pi(1 + g^2\lambda^2/2)}}\tau e^{\tau}(1 \pm \mathbf{i}) \right). \quad (19)$$

The stability of the solution 0 is governed by the sign of the real part of the uppermost eigenvalue. There can be an infinite number of characteristic roots of the equations, but for any real ν_0 there exists a finite number such that $\Re(\zeta) > \nu_0$. The eigenvalue with largest real part is given by the real branch W_0 , and if the argument has a real part greater than $-e^{-1}$ the root is unique. If this is not the case, two eigenvalues have the same real part, namely the ones corresponding to $k = 0$ or $k = -1$.

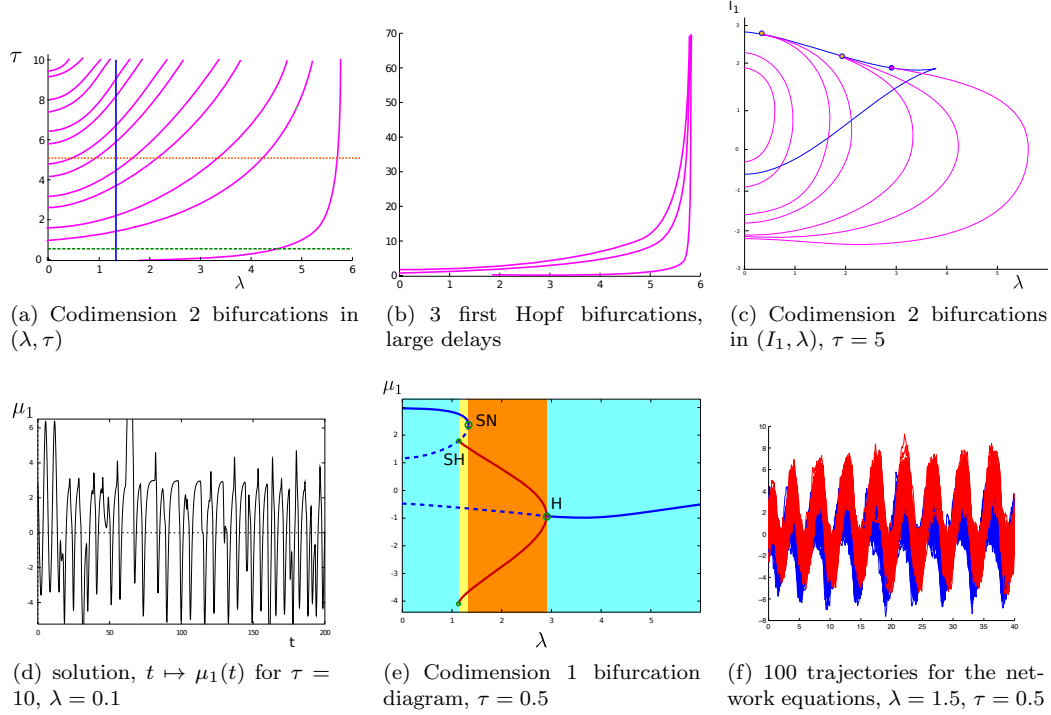


Figure 2: Dynamics and bifurcations of the mean-field equations (11). (a): Codimension 2 bifurcation diagram as a function of the noise intensity λ and the delay τ : saddle-node bifurcations (blue line) and cascade of Hopf bifurcation (pink curves) that all have a common vertical asymptote (b). (c): Codimension 2 bifurcation diagram as a function of I_1 and λ for $\tau = 0.5$ (green line in diagram (a)): 2 degenerate bifurcations appear, corresponding to the tangential merging of two Hopf with the saddle-node bifurcation, and one Bogdanov-Taken bifurcation. (d) Codimension 1 bifurcation diagram as a function of the noise intensity λ and $I_1 = 0$, segmented into three zones: blue for stationary solution, yellow for bistability between a stationary/ periodic solutions, and orange: periodic behavior. In the periodic region, all neurons in the network are synchronized (2(f): blue (resp. red): 50 trajectories from neurons of the excitatory (resp. inhibitory) population 1 (resp. 2)). The diagrams were obtained using DDE-BIFTOOL [51, 52] and a specific code for the network equations.

We observe that the argument of the Lambert function in the expression (19) has a modulus that decreases towards 0 as λ or τ are increased towards infinity. For fixed values of τ , the rightmost eigenvalue is given by $k = 0$, we hence observe that as λ is increased, the value of W_0 decreases towards 0, and there exists a value $\lambda(\tau)$ such that for any $\lambda > \lambda^*(\tau)$ the fixed point 0 is stable: noise has a stabilizing effect on this fixed point. This stabilization appears through a Hopf bifurcation, and periodic behaviors are found for $\lambda < \lambda^*(\tau)$, as shown in the bifurcation diagram 3(e) for a fixed value of the delays, $\tau = 0.5$. For fixed values of λ , as τ is increased, the real parts of the eigenvalues increase and might switch from positive to negative (see figure 3(a)). As delays are increased, a growing number of eigenvalues have positive real part, which accounts for the more complex phenomena of creation and destruction of limit cycles and for the increasing number of fixed points as a function of λ and τ .

Let us now investigate more thoroughly the location of possible Hopf bifurcations. These are necessarily points where the real part of the characteristic roots vanishes. Following [48, 54], we use the fact that a necessary condition for the existence of a Hopf bifurcation is the existence of a purely imaginary characteristic root $\zeta = i\omega$. This condition, plugged into formula (18) yields the condition:

$$-(i\omega + 1) = -\frac{g}{\sqrt{2\pi(1 + g^2\lambda^2/2)}}e^{-i\omega\tau}(1 \pm i) \quad (20)$$

which, taking the squared modulus of these imaginary numbers, give the equality:

$$1 + \omega^2 = \frac{g^2}{\pi(1 + g^2\lambda^2/2)}$$

i.e.

$$\omega^2 = \frac{-\pi + g^2(1 - \pi\lambda^2/2)}{\pi(1 + g^2\lambda^2/2)}. \quad (21)$$

This quantity is necessary positive, hence Hopf bifurcations only arise for values of the noise intensity satisfying the inequality:

$$\lambda^2 \leq (\lambda^*)^2 \stackrel{\text{def}}{=} 2 \left(\frac{1}{\pi} - \frac{1}{g^2} \right).$$

This inequality precisely corresponds to the vertical asymptote: for any value of the noise intensity greater than λ^* , no Hopf bifurcation is possible in the system. This property indicates that necessarily, for noise intensities greater than λ^* , the fixed point $(0, \lambda^2/2)$ is stable. Indeed, we already mentioned that for large noise values that fixed point is stable. It can gain stability only if the real part of one of the characteristic roots crosses the imaginary axis, corresponding either to purely imaginary roots or null roots, and the previous inequality showed that such roots do not exist for parameters $\lambda > \lambda^*$.

Under the condition $\lambda < \lambda^*$, we can perfectly characterized Hopf bifurcations by equating the argument of both sides of equality (20). We obtain that way:

$$\tau = \frac{-\arctan(\omega) \pm \frac{\pi}{4} + 2k\pi}{\omega}$$

for $k \in \mathbb{Z}$. This relationship can be written in closed form as a function of the parameters using the expression of ω obtained in equation (21). The different curves of Hopf bifurcations

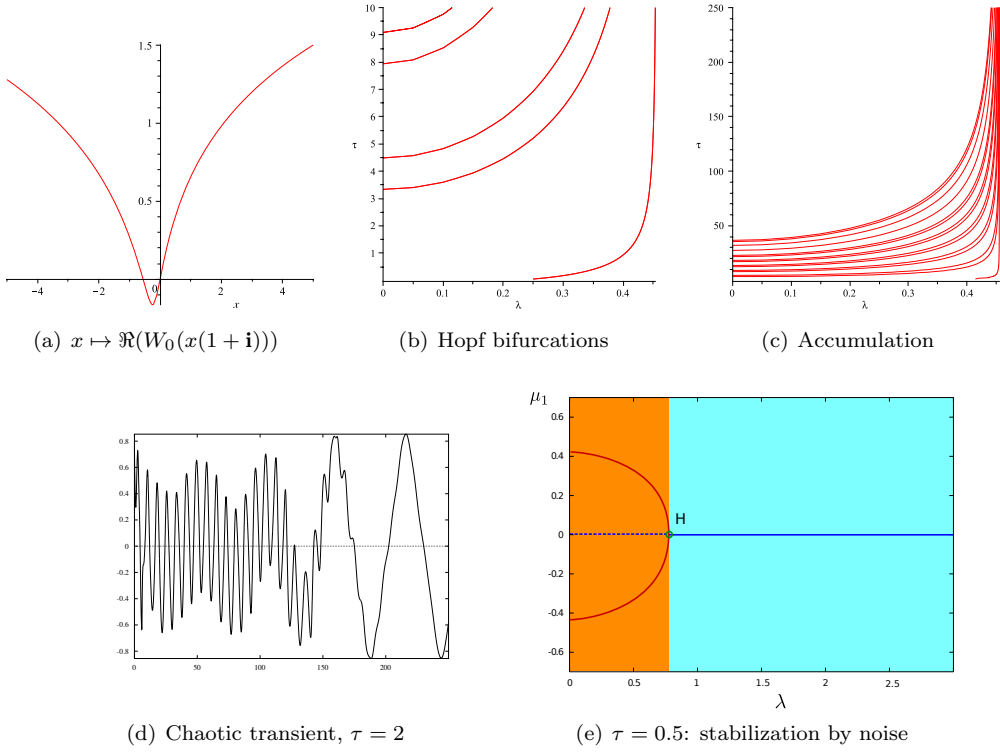


Figure 3: Analysis of the characteristic roots of the delayed neural field equations related to the equilibrium point $\mu_1 = \mu_2 = 0$ and $v_1 = v_2 = \lambda^2/2$. Results are similar to those of Fig. 2: as delays are increased, several Hopf bifurcations arise and accumulate around the same value. (a): Shape of the Lambert function $x \mapsto \Re(W_0(x(1+i)))$, (b): cascade of Hopf bifurcations and (c): locus of the Hopf bifurcations for the 15 first characteristic root continued for very large values of τ (d): Transient regime for $\tau = 5$ and (e): Bifurcation diagram as a function of λ for $\tau = 0.5$.

are plotted in Figure 3. We observe the exact same phenomenon of cascade, accumulation and pairing of Hopf bifurcations as delays are increased. The accumulation is related to the fact that the value of λ related to a Hopf bifurcation increases as a function of τ , and that the value of λ is upperbounded. This case again is characterized, for large values of τ , by the presence of irregular transient behaviors corresponding to the very complex landscape of the phase plane, as displayed in Fig. 3(d). We chose for instance to display the transient solution for $\tau = 4$, a case where the delays are small enough so that we can resolve the presence of different limit cycles trapping the solution transiently. This case hence makes explicit the dependence on noise levels of qualitative behaviors of the system for finite populations networks. We now extend the study to infinite populations networks in a neural field setting.

4.2. Neural Fields Dynamics

We now turn our attention to the study of the dynamics of the neural field equations derived in section 3.2. We start by an analytic study of the dynamics of a single layer neural field with delays with a particular focus on Turing-Hopf bifurcations from spatially

homogeneous states, before addressing numerically the same questions in the more complex and more relevant dynamics of a two-layers neural field composed of an excitatory and an inhibitory layers.

4.2.1. A single layer neural field: Turing-Hopf instabilities and noise

In this section, we consider the case of a single-layer neural field, whose mean and standard deviation satisfy equations (15). In order to analyze the dynamics of the solutions, we chose a particular set of parameters that allow analytical studies. We consider a one-dimensional periodic neural field on $\Gamma = \mathbb{S}^1$ distributed homogeneously (i.e. $\lambda(x) = 1$), with connectivity functions $J(r, r')$ and $\sigma(r, r')$ only depending on $|r - r'|$, $\theta(r)$ constant, and denote with a slight abuse of notation θ the constant value of the function $\theta(r)$, $J(r, r') = J(r - r')$ (resp. $\sigma(r, r') = \sigma(r - r')$). We denote by \mathcal{J} (resp. $\tilde{\sigma}^2$) the integral $\int_0^1 J(r, r') dr'$ (resp. $\int_0^1 \sigma^2(r, r') dr'$) assumed finite (these obviously do not depend on r). Taking $S(r, x) = \text{erf}(gx)$, the function $f(r, x, y)$ is equal, as already stated, to $\text{erf}(gx/\sqrt{1+g^2y})$. Hence $F_0 \stackrel{\text{def}}{=} f(r, 0, v)$ does not depend on v . Let us further set $I = -\mathcal{J}F_0$. In that case, $\mu(r, t) \equiv 0$ for any $(r, t) \in \Gamma \times \mathbb{R}^+$ is a solution of the mean equation whatever the standard deviation v is, and this variable v is solution of the equation:

$$\frac{\partial v}{\partial t}(r, t) = -\frac{2}{\theta} v(r, t) + \tilde{\sigma}^2 F_0^2 + \Lambda^2(r, t).$$

Let us further assume that $\Lambda(r, t)$ is constant. Then the spatially homogeneous, constant in time function:

$$(\mu(r, t), v(r, t)) \equiv \left(0, \frac{\theta}{2}(\tilde{\sigma} F_0^2 + \Lambda^2)\right) \stackrel{\text{def}}{=} (\mu_0, v_0)$$

is solution of the neural field equations.

It is clear that since the domain is periodic and both the connectivity and the delay functions only depend on $|r - r'|$, the related neural field satisfies the full synchronization property of proposition 3. The spatially homogeneous state (or synchronized state) satisfies the equations:

$$\begin{cases} \frac{d\mu}{dt} = -\frac{\mu}{\theta} + \int_0^1 J(r) f(\mu(t - \tau(r)), v(t - \tau(r))) dr + I \\ \frac{dv}{dt} = -\frac{2v}{\theta} + \int_0^1 \sigma^2(r) f^2(\mu(t - \tau(r)), v(t - \tau(r))) dr + \Lambda^2 \end{cases}$$

which is a delayed differential equation that is formally equivalent to a differential equation with delays distributed on the interval $[\min_r \tau(r), \max_r \tau(r)]$ with the density $J(r)$. The spatially homogeneous equilibria $(\bar{\mu}, \bar{v})$ are hence solution of the equations:

$$\begin{cases} -\frac{\bar{\mu}}{\theta} + \tilde{J}f(\bar{\mu}, \bar{v}) + I & = 0 \\ -\frac{2\bar{v}}{\theta} + \tilde{\sigma}^2 f^2(\bar{\mu}, \bar{v}) + \Lambda^2 & = 0 \end{cases}$$

and are obviously the same equilibria as for the non-delayed spatially homogeneous equations:

$$\begin{cases} \frac{d\mu}{dt} = -\frac{\mu}{\theta} + \tilde{J}f(\mu, v) + I \\ \frac{dv}{dt} = -\frac{2v}{\theta} + \tilde{\sigma}^2 f^2(\mu, v) + \Lambda^2 \end{cases}$$

The bifurcation diagram of this non-delayed system as a function of the slope of the noise Λ is produced in Figure 4. If the slope g is small enough (precisely $g < \sqrt{2\pi/\mathcal{J}}$), the fixed

point (μ_0, v_0) is the unique fixed point and is always stable whatever the noise parameters are. For larger values of g (in Fig. 4 we chose $g = 3$), the system presents two distinct regimes as a function of the noise parameters: for small values of the parameters σ and Λ , the system presents three fixed points, (μ_0, v_0) that is unstable and two distinct fixed points denoted (μ_1, v_1) and (μ_2, v_2) which are stable, and that hence constitute spatially homogeneous and constant in time solutions of the mean-field equations. The system undergoes a pitchfork bifurcation on the manifold defined by $\tilde{\sigma}^2 F_0^2 + \Lambda^2 = -1/g^2 + \mathcal{J}/2\pi$, and on this line the two fixed points (μ_1, v_1) and (μ_2, v_2) collapse with (μ_0, v_0) and disappear. For σ and Λ such that $\tilde{\sigma}^2 F_0^2 + \Lambda^2 > -1/g^2 + \mathcal{J}/2\pi$ system is left with a unique equilibrium, (μ_0, v_0) , which is now stable. Hence again appears a stabilization effect of noise on the spatially homogeneous fixed point (μ_0, v_0) .

Let us now return to the full spatially extended system with delays, and address the problem of pattern formation in these equations beyond a Turing instability at the spatially homogeneous steady state (μ_0, v_0) . To this purpose, we analyze the linear stability of this fixed point (see e.g. [55, 56, 46]), which amounts characterizing the eigenvalues of the linearized equations around this fixed point. Since $f(x, y) = \text{erf}(gx/\sqrt{1+g^2y})$, we clearly have:

$$\begin{cases} \frac{\partial f}{\partial x}|_{(\mu_0, v_0)} = \frac{g}{\sqrt{1+g^2v_0}} \frac{1}{\sqrt{2\pi}} \stackrel{\text{def}}{=} F'_0 \\ \frac{\partial f}{\partial y}|_{(\mu_0, v_0)} = \frac{-g^3\mu_0}{\sqrt{\pi(1+g^2v_0)^3}} e^{-\frac{\mu_0^2 g^2}{1+g^2v_0}} = 0 \end{cases}$$

and hence the linearized equations around (μ_0, v_0) read:

$$\begin{cases} \frac{\partial A}{\partial t}(r, t) &= -\frac{1}{\theta} A(r, t) + F'_0 \int_{\Gamma} J(r' - r) A(r', t - \tau(r' - r)) dr' \\ \frac{\partial B}{\partial t}(r, t) &= -\frac{2}{\theta} B(r, t) + 2F_0 F'_0 \int_{\Gamma} \sigma^2(r' - r) A(r', t - \tau(r' - r)) dr' \end{cases}$$

We recall that the integral operators are convolutions on \mathbb{S}^1 , these can hence be diagonalized on the Fourier basis. Let us consider perturbations of the equilibrium of the form $A_{\nu, k}(r, t) = \Re(e^{\nu t + 2\pi k r})$ with $\nu = i\omega + l$, and leave $B(r, t)$ unspecified. Let us denote by $(a_k(\nu))$ and $(b_k(\nu))$ the Fourier coefficients of the functions $J(r)e^{-\nu\tau(r)}$ and $\sigma(r)e^{-\nu\tau(r)}$:

$$\begin{cases} a_k(\nu) &= \int_{\Gamma} J(r') e^{-\nu\tau(r')} e^{-2i\pi k r'} dr' \\ b_k(\nu) &= \int_{\Gamma} \sigma^2(r') e^{-\nu\tau(r')} e^{-2i\pi k r'} dr' \end{cases}$$

The functions $A_{\nu, k}$ are eigenfunctions for the first equation the linearized system provided that ν satisfies the relationship:

$$\nu = \nu_k \stackrel{\text{def}}{=} -\frac{1}{\theta} + F'_0 a_k,$$

defining a *dispersion relationship*. The characteristic roots of the linearized equations is hence composed of the eigenvalues of the matrix:

$$\begin{pmatrix} -\frac{1}{\theta} + F'_0 a_k & 0 \\ 2F_0 F'_0 b_k & -2/\theta \end{pmatrix}$$

which are exactly $\{-2/\theta, -1/\theta + F'_0 a_k, k \in \mathbb{N}\}$. In particular, this shows that no instability can occur on the standard deviation equation, and the whole stability of the homogeneous

fixed point only depends on the Fourier coefficients of the deterministic connectivity function multiplied by the exponential of the delay function, $J(r)e^{-\tau(r)}$, and on the quantity F'_0 which depends on the different parameters of the system. Explicitly, in the original parameters, the spectrum is hence composed of the eigenvalues $\{-\frac{2}{\theta}, -\frac{1}{\theta} + a_k \frac{g}{\sqrt{2\pi(1+g^2v_0)}}, k \in \mathbb{N}\}$ with $v_0 = \frac{\theta}{2}(\tilde{\sigma}F_0^2 + \Lambda^2)$. Let a_M be the largest Fourier coefficient of J : $a_M = \max_{k \in \mathbb{N}} a_k$. By our integrability assumption on J , this maximum necessarily exists because of Parseval-Plancherel theorem. The solution $(0, v_0)$ is hence linearly stable as soon as $-1/\theta + a_M g/\sqrt{2\pi} < 0$.

This particular form of the spectrum of the linearized operator quantifies directly a stabilization effect of the noise already mentioned. Indeed, let us assume that θ and g are fixed. If $-1/\theta + \alpha g/\sqrt{2\pi} < 0$, then all the eigenvalues are negative whatever v_0 and hence the solution $(0, v_0)$ is stable whatever the noise connectivity matrix σ and the additive noise Λ . If now $-1/\theta + \alpha g/\sqrt{2\pi} > 0$, then for Λ and σ small, the fixed point $(0, v_0)$ is unstable. When σ or Λ are increase, the fixed point will gain stability, since the maximal eigenvalue tends to $-1/\theta$ when v_0 goes to infinity⁴.

An instability occurs when the characteristic roots such that ν has a positive real part. A Turing bifurcation point is defined by the fact that there exists an integer k such that $\Re(\nu_k) = 0$. It is said to be *static* if at this point $\Im(\nu_k) = 0$, and *dynamic* if $\Im(\nu_k) = \omega_k \neq 0$. In that latter case, the instability is called Turing-Hopf bifurcation, and generates a global pattern with wavenumber k moving coherently at speed ω_k/k as a periodic wavetrain. If the maximum of λ_k is reached for $k = 0$, another homogeneous is excited.

In order to investigate the presence of Turing-Hopf instabilities, we specify further our system. We choose an exponential connectivity function $J(r) = e^{-|r|/s}$ for some $s > 0$, and a delay taking into account both propagation (or axonal) delays corresponding to the transport of the information along the axons at a constant finite speed c , and constant delays accounting for the transmission time of the spike through the synaptic machinery. In that case,

$$\tau(r) = \frac{|r|}{c} + \tau_d.$$

The coefficient $a_k(\nu)$ hence read:

$$\frac{e^{-\nu\tau_d}(1 - e^{-(\frac{1}{s} + \frac{\nu}{c})})}{\frac{1}{s} + \frac{\nu}{c} + \mathbf{i}2\pi k}$$

The related characteristic equation reads:

$$\nu + \frac{1}{\theta} = F'_0 \frac{e^{-\nu\tau_d}(1 - e^{-(\frac{1}{s} + \frac{\nu}{c})})}{\frac{1}{s} + \frac{\nu}{c} + \mathbf{i}2\pi k}$$

These equations are relatively complex to solve analytically in that general form (see e.g. [57]). However, when considering purely synaptic delay case (corresponding formally to $c = \infty$, i.e. disregarding the transport phenomenon), a similar analysis as the one performed in the previous section allows computing in closed form the curves of Turing-Hopf instabilities.

⁴The stabilization effect already mentioned in previous examples comes from the fact that noise tends to make the sigmoidal transform less sharp, which explicitly appears in our equations, since the slope of the effective sigmoidal transform reads $g/\sqrt{2\pi(1+g^2v_0)}$ which is always smaller than the slope of the sigmoid that intervenes in the deterministic case, $g/\sqrt{2\pi}$, and which decreases as noise is increased.

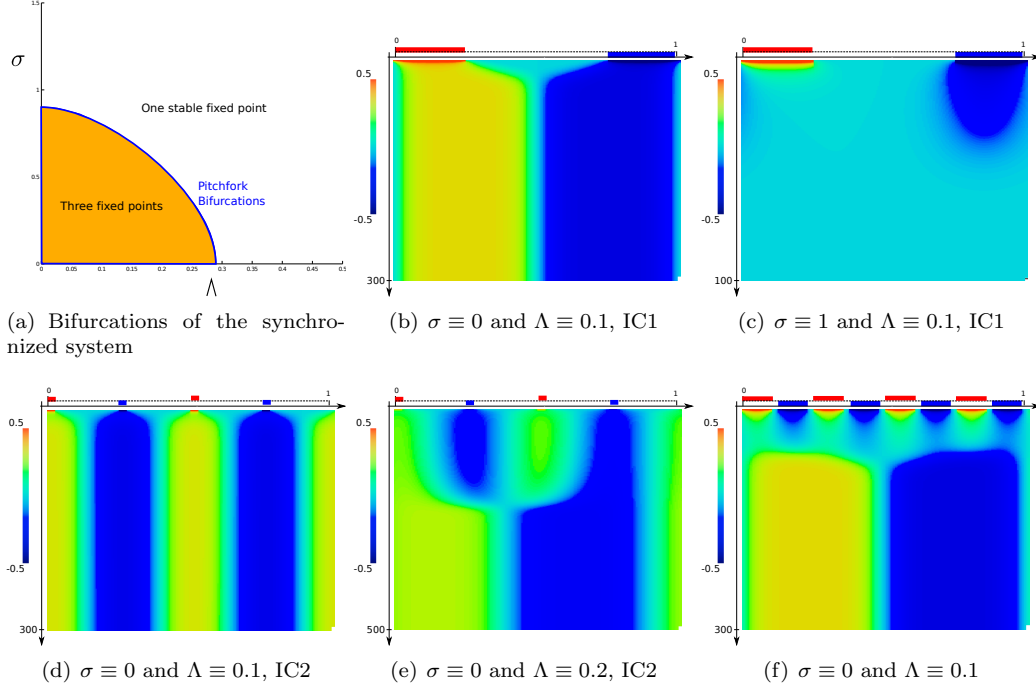


Figure 4: Stabilization by noise of the spatially homogeneous state (μ_0, v_0) . (a) shows the bifurcation diagram as a function of σ and Λ of the fully synchronized state, (b): for initial conditions IC1 given by (22) and small noise levels, the system stabilizes on a non-spatially homogeneous state (mode $k = 1$) but for larger values of Λ (not shown) or σ (c) the state (μ_0, v_0) is stabilized and attractive. (d): same thing for initial conditions IC2 given by (23) shows mode $k = 2$ excited, and as Λ is increased (e), this state loses stability in favor of the mode $k = 1$ before (μ_0, v_0) is stabilized. (f) shows the instability of the mode related to $k = 4$.

Dynamical instabilities occur for parameters such that: $\frac{F_0'^2(1-e^{-1/s})^2}{1/s^2+4\pi^2k^2} > \frac{1}{\theta^2}$. In that case, let us denote by ω_k the quantity:

$$\omega_k = \sqrt{\frac{F_0'^2(1-e^{-1/s})^2}{\frac{1}{s^2} + 4\pi^2k^2} - \frac{1}{\theta^2}}$$

the instability arises for parameters such that there exists $m \in \mathbb{Z}$ for which is valid the relationship:

$$\tau_d^k = \frac{1}{\omega_k} \left(-\arctan(\theta\omega_k) - \arctan(2\pi ks) + 2\pi m \right).$$

Let us now numerically explore the bifurcations of this system. We aim at exhibiting different solutions that are not spatially homogeneous, corresponding to different wavenumbers, and to this end specify particular initial conditions. We have seen that for small values of the noise parameters and large values of the slope g , the fully synchronized system presented two different stable equilibria that we denoted (μ_1, v_1) and (μ_2, v_2) . If all initial conditions belong to the attraction bassin of the same stable fixed point, or are equal to zero, then the only mode to be excited corresponds to $k = 0$, and the neural field stabilizes on a

constant mode. If we now partition Γ into different connected zones and set up the initial condition so that neurons belonging to different subsets of Γ belong to the attraction bassin of the two different stable fixed points, in a balanced manner, higher modes are excited. As examples, setting the initial condition to:

$$\mu(r, t) = \begin{cases} 1 & r \in [0, 0.25], t \in [-\tau, 0] \\ -1 & r \in [0.75, 1], t \in [-\tau, 0] \\ 0 & \text{otherwise} \end{cases} \quad (22)$$

we excite a non-constant mode $k = 1$ as illustrated in Fig. 4(b), and setting the initial condition to:

$$\mu(r, t) = \begin{cases} 1 & r \in [0, 0.05] \cup [0.5, 0.55], t \in [-\tau, 0] \\ -1 & r \in [0.25, 0.3] \cup [0.75, 0.8], t \in [-\tau, 0] \\ 0 & \text{otherwise} \end{cases} \quad (23)$$

we excite the mode $k = 2$, as illustrated in Fig. 4(d). In these plots, the abscissa represents the location on the space Γ and the ordinate corresponds to time. As noise is increased, this mode loses stability in favor of the mode $k = 1$ first, before this mode loses again stability in favor of the spatially homogeneous solution (μ_0, v_0) as expected from the analysis of the stability of that fixed point. Higher modes prove relatively unstable, and illustrated in Fig. 4(f) for an initial condition corresponding to a wavenumber $k = 4$. After a short transient, the system stabilizes on a stationary solution corresponding to the mode $k = 1$.

For axonal delays, the characteristic equation obtained is very complicated to solve analytically. These are simplified when considering wizard hat connectivity kernels, as shown in [46]. We can however obtain complex closed form expressions of the Turing-Hopf bifurcation curves using [57]. These are not made explicit here, and simulations performed using an adaptation of the code provided by Venkov in [58] yield very similar phenomena (not shown).

The dynamic Turing bifurcations in the particular one-layer case treated, chosen for simplifying analytical exploration, presented a limited set of spatio-temporal behaviors: we observed that only stationary solutions are found, either spatially homogeneous or characterized by a few typical modes. In particular, no wave or oscillatory activity was observed, because of our particular choice of connectivity function which was chosen of constant sign (here, positive) for biological reasons. In order to go beyond these behaviors, we now turn to the numerical study of a more complex neural field system composed of two layers in order to include both excitation and inhibition phenomena. We will observe in these cases complex irregular dynamic Turing patterns are observed in a particular range of noise levels.

4.2.2. Dynamic Turing patterns in a two layers neural field with periodic boundary conditions

We now consider a two layers neural field composed of an excitatory (labeled by the index 1) and an inhibitory (labeled by an index 2) populations distributed over the space $\Gamma = \mathbb{S}^1$ or $\Gamma = [0, 1]$. Both layer produce currents sent to both the excitatory and the inhibitory layers, and the interconnection strength depends on the (functional or anatomical) distance between themselves in Γ (see e.g. [59]). We consider here constant sign connectivities with an exponential shape, with a width depending on the population: $J_a(r, r') = e^{-|r-r'|/s_a}/s_a$ for $a = 1$ or 2 . The choice of the typical spatial extension of the kernel depends on type of modeling chosen. For instance, if one considers that Γ is a functional space (i.e. each $r \in \Gamma$

corresponds to a function of the population, for instance the preferred orientation of the column), then local interactions are dominated by excitation and the connection between two very distinct functions (e.g. orientations) are dominated by inhibition, which motivates a choice $s_1 > s_2$. If Γ models the spatial location of each neuron, it is known that inhibitory connections are generally characterized by shorter axons and excitatory synapses project their synapses further, which would motivate a choice of typical sizes such that $s_2 > s_1$.

In the present section, we consider *periodic* boundary condition. This choice hence is close from functional neural fields settings, and for instance classically models orientation preference. The neural field can be seen as defined on the torus \mathbb{S}^1 . Two other types of connectivity will be dealt with in [Appendix B](#): (i) *reflective* boundary conditions in which the solution is virtually evenly continued at the boundaries 0 and 1 and the convolution is done on \mathbb{R} instead of $[0, 1]$ and (ii) *zero* boundary conditions where the convolution only occurs on $[0, 1]$ (which would correspond to a convolution on \mathbb{R} with a null continuation outside the interval $[0, 1]$).

We define the type function of a neuron (excitatory or inhibitory) by the function $\nu(i) \in \{1, 2\}$. The connectivity kernels J_ν are multiplied by a typical connectivity coefficient between the different populations, $w_{\nu\nu'}$ for the deterministic interactions, chosen, consistently with the previous finite-population example, equal to:

$$w = \begin{pmatrix} 15 & -12 \\ 16 & -5 \end{pmatrix}.$$

Noisy interaction $\sigma_{\nu,\nu'}(r, r')$ are considered equal to a coefficient $\sigma_{\nu,\nu'}$ multiplied by the exponential kernels $J_{\nu'}(r, r')$, and the typical time constants $\theta_\nu(r)$ of all neurons is considered equal to 1. In a network composed of $N_{\gamma\nu}$ neurons of type ν in the population located at $r_\gamma \in \Gamma$, the equation of neuron i of type $\nu(i) = a \in \{1, 2\}$, in population α at location r_α reads:

$$\begin{aligned} dV^i(t) = & \left(-V^i(t) + I_a(r_\alpha, t) + \sum_{\gamma=1}^{P(N)} \sum_{\nu=1}^2 \frac{1}{N_{\gamma\nu}} \sum_{j, p(j)=\gamma, \nu(j)=\nu} w_{a\nu} J_\nu(r_\alpha, r_\gamma) S(r_\gamma, V^j(t - \tau(r_\alpha, r_\gamma))) \right) dt \\ & + \sum_{\gamma=1}^{P(N)} \sum_{\nu=1}^2 \frac{1}{N_{\gamma\nu}} \sum_{j, p(j)=\gamma, \nu(j)=\nu} \sigma_{a\nu} J_\nu(r_\alpha, r_\gamma) S(r_\gamma, V^j(t - \tau(r_\alpha, r_\gamma))) dB_t^{\alpha, a, \gamma, \nu} + \Lambda(r_\alpha, t) dW_t^i \end{aligned}$$

A straightforward multi-dimensional extension of theorem 2 and proposition 6 allows proving that the same propagation of chaos property applies, deriving the stochastic mean-field equations, proving that the solutions of these are Gaussian, with mean and covariances

satisfying the coupled equations:

$$\begin{cases} \frac{\partial \mu_1}{\partial t}(r, t) &= -\mu_1(r, t) + \int_{\Gamma} \lambda(r') dr' \left\{ w_{11} J_1(r, r') f(r, \mu_1(r', t - \tau(r, r')), v_1(r', t - \tau(r, r'))) \right. \\ &\quad \left. + w_{12} J_2(r, r') f(r, \mu_2(r', t - \tau(r, r')), v_2(r', t - \tau(r, r'))) \right\} + I_1(r, t) \\ \frac{\partial \mu_2}{\partial t}(r, t) &= -\mu_2(r, t) + \int_{\Gamma} \lambda(r') dr' \left\{ w_{21} J_1(r, r') f(r, \mu_1(r', t - \tau(r, r')), v_1(r', t - \tau(r, r'))) \right. \\ &\quad \left. + w_{22} J_2(r, r') f(r, \mu_2(r', t - \tau(r, r')), v_2(r', t - \tau(r, r'))) \right\} + I_2(r, t) \\ \frac{\partial v_1}{\partial t}(r, t) &= -2 v_1(r, t) + \int_{\Gamma} \lambda(r')^2 dr' \left\{ \sigma_{11}^2 J_1^2(r, r') f^2(r, \mu_1(r', t - \tau(r, r')), v_1(r', t - \tau(r, r'))) \right. \\ &\quad \left. + \sigma_{12}^2 J_2^2(r, r') f^2(r, \mu_2(r', t - \tau(r, r')), v_2(r', t - \tau(r, r'))) \right\} + \Lambda_1^2(r, t) \\ \frac{\partial v_2}{\partial t}(r, t) &= -2 v_2(r, t) + \int_{\Gamma} \lambda(r')^2 dr' \left\{ \sigma_{21}^2 J_1^2(r, r') f^2(r, \mu_1(r', t - \tau(r, r')), v_1(r', t - \tau(r, r'))) \right. \\ &\quad \left. + \sigma_{22}^2 J_2^2(r, r') f^2(r, \mu_2(r', t - \tau(r, r')), v_2(r', t - \tau(r, r'))) \right\} + \Lambda_2^2(r, t) \end{cases} \quad (24)$$

We numerically explore the solutions of these equations and the dependence upon noise, initial datum and boundary conditions on the neural field. We further simplify the problem by considering that the additive noise parameters $\Lambda_1(r, t)$ and $\Lambda_2(r, t)$ are identical and constant, and denote their common value Λ . Similarly, we assume that $\sigma_{\nu\nu'}$ are all equal to a quantity denoted σ . The (space-dependent) delays are neglected in the present study, i.e. set $\tau(r, r') \equiv 0$. Their specific influence will be analyzed in a separate study.

Since the connectivity matrix is convolutional and the domain is periodic, the system clearly satisfies the total synchronization condition given in equation (6), and we expect to find spatially homogeneous solutions when the initial conditions are themselves spatially homogeneous. Let us denote by \mathcal{J}_a the quantity:

$$\mathcal{J}_a = \int_{\Gamma} \lambda(r') dr' J_a(r, r')$$

and by $\tilde{\mathcal{J}}_a^2$:

$$\tilde{\mathcal{J}}_a^2 = \int_{\Gamma} \lambda(r')^2 dr' J_a^2(r, r')$$

for $a \in \{1, 2\}$. The infinite dimensional system (24) reduces, when considering its spatially homogeneous solutions, to the 4-dimensional ordinary differential equation:

$$\begin{cases} \dot{\mu}_1 &= -\mu_1 + w_{11} \mathcal{J}_1 f(\mu_1, v_1) + w_{12} \mathcal{J}_2 f(\mu_2, v_2) + I_1(t) \\ \dot{\mu}_2 &= -\mu_2 + w_{21} \mathcal{J}_1 f(\mu_1, v_1) + w_{22} \mathcal{J}_2 f(\mu_2, v_2) + I_2(t) \\ \dot{v}_1 &= -2 v_1 + \sigma^2 \left(\tilde{\mathcal{J}}_1^2 f^2(\mu_1, v_1) + \tilde{\mathcal{J}}_2^2 f^2(\mu_2, v_2) \right) + \Lambda_1^2 \\ \dot{v}_2 &= -2 v_2 + \sigma^2 \left(\tilde{\mathcal{J}}_1^2 f^2(\mu_1, v_1) + \tilde{\mathcal{J}}_2^2 f^2(\mu_2, v_2) \right) + \Lambda_2^2 \end{cases} \quad (25)$$

Functional Connectivity Case. We start by considering a case where $s_1 > s_2$, which is related as stated to functional connectivity: local interactions are governed by excitation and distal interconnections by inhibition. We fix $s_1 = 0.02$ and $s_2 = 0.0125$. Figure 5 represents the bifurcation diagram of the fully-synchronized system for $I_1 = 0$ and $I_2 = -3$, as a function of the additive noise amplitude $\Lambda_1 = \Lambda_2 = \Lambda$, and of the constant common synaptic noise amplitude $\sigma = \sigma_{\nu\nu'}$. The codimension two bifurcation diagram presents a Hopf, a saddle-node and a saddle-homoclinic bifurcation curves, separating the diagram

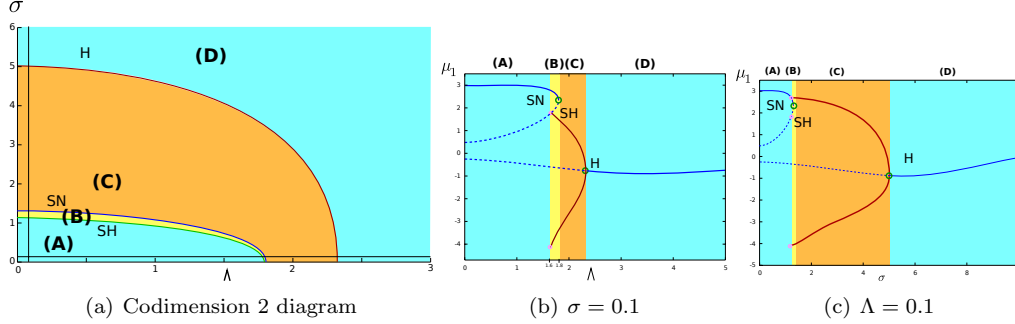


Figure 5: Bifurcation diagram of the fully synchronized state. (a) Codimension 2 bifurcation diagram with respect to σ and Λ presents three bifurcations manifolds: saddle-homoclinic (SH, green), saddle-node (SN, blue) and Hopf (H, brown) separating the bifurcation diagram into 4 zones: two stationary (cyan, A and D), a periodic zone (C, orange) and a bistable zone (B, yellow). Codimension 1 bifurcation diagram as a function of Λ or σ for fixed values of the other noise parameter are displayed in (b) and (c).

into three qualitatively distinct zones: two stationary zone (A and D, colored in cyan) where the moment system presents a stable fixed point, i.e. the solution of the mean-field equation is stationary, separated by the saddle-homoclinic bifurcation curve from a bistable zone (B, yellow) where the moment equations present both a stable fixed point and a periodic orbit, and a zone where there only exists a periodic orbit (C, orange). The bistable zone is separated from the periodic behavior zone through a saddle-node bifurcation, and the periodic behavior zone from the stationary zone (D) through a Hopf bifurcation. The analysis of this diagram underlines the similar but asymmetrical role of σ and Λ . As examples we plotted codimension 1 bifurcation diagrams for $\Lambda = 0.1$ as a function of σ and for $\sigma = 0.1$ as a function of Λ (black lines in the codimension two diagram). We observe that for small noise amplitude (either σ or Λ) corresponding to parameter region (A), the system presents a stable high fixed point and two unstable fixed points, a saddle and a repulsive fixed point. As this noise parameter is further increased, a cycle appears from the saddle fixed point through a saddle homoclinic bifurcation, and we enter the bistable (yellow) region (B). As noise is further increased, the stable and the saddle fixed point merge and disappear through a saddle-node bifurcation, and the system is left with an unstable fixed point and a stable periodic orbit (region C). This orbit decreases amplitude disappears through a Hopf as noise is increased, and at this bifurcation the unstable fixed point gains stability (region D).

The diagrams presented in Figure 5 characterize the existence and the nature of the synchronized states. As soon as the initial condition is homogeneous, the system will present solutions that are constant in space, and their time profile is given by the solutions of the fully-synchronized system. However, these synchronized states might not be stable, and inhomogeneities in the initial condition might lead the system to different states. Bifurcations from these spatially homogeneous states could be analytically as outlined in the previous section. However, due to the dimensionality of the system and to the particular coefficients chosen, the equilibria are complicated to characterize and hence the analytical characterization of Turing-Hopf bifurcations is here intricate. This is why we address that problem numerically by computing the solutions of the neural-field moment equation for different values of the parameter Λ or σ , with homogeneous or inhomogeneous initial condition. Re-

sults are displayed in Figures 6 and 7. In these figures is plotted the mean of the activity of the excitatory population, $\mu_1(r, t)$, as a function of r (abscissa) and t (ordinate).

The behaviors identified through the bifurcation analysis of the synchronized equations are perfectly recovered in the analysis of the neural field when taking an homogeneous initial condition, as expected from proposition 3. The stability of these synchronized states is analyzed through perturbations of the synchronized initial condition. Let us start by analyzing the effect of the parameter Λ for a fixed value of $\sigma = 0.1$. In the stationary regime (A) corresponding to low noise amplitudes, very intricate phenomena take place that tend to destabilize the spatially homogeneous solutions. Let us fix for instance the initial condition of $\mu_1(r)$ to 5 for $r \in [0, 0.05]$ and 0 otherwise⁵. If the noise is small enough, the initial condition creates bi-directional waves that travel through the neural field. These waves split into different secondary waves, themselves potentially splitting. All these waves interact together, and this phenomenon results in highly irregular transient behaviors (see e.g. Fig. 6(a) for $\Lambda = 0.1$). This wave splitting and interaction phenomenon becomes sustained in time as Λ is further increase. For our parameters, the wave splitting and interaction phenomenon is sustained for $\Lambda \geq 1$. Figure 6(d) illustrates this behavior for $\Lambda = 1$. From the analysis of the spatio-temporal patterns, we observe the fact that waves tend to spread increasingly fast across the neural field as noise is increased. The irregular pattern suddenly turn as noise is further increased into a space-time quasi-periodic waves. These states, presented in Fig. 6(f), show more regular quasi-periodic spatial patterns that oscillate quasi-periodically in time. These waves appear not to interfere together, which explains the increased regularity observed in contrast with the patterns observed for smaller values of the noise parameter. These are present for increasing values of Λ until the bistable parameter region (B) is reached.

For noise levels corresponding to the bistable region (B) or to the oscillatory region (C), it appears that the spatially homogeneous periodic regime is attractive: for non-homogeneous initial conditions, the system smoothly goes from a non-synchronized irregular activity to spatially homogeneous time-periodic activity corresponding to the spatially homogeneous solution of system (25) identified, see Figure 7(a). In the bistable region (B), one may wonder if similarly to the case of section 4.2.1, the presence of two stable equilibria could excite higher wavenumber. In order to numerically investigate this question we set up the initial condition at equilibrium for one part of the neural field and on the limit cycle for the other part. In the extensive numerical tests performed, we always obtained that the oscillatory regime would take over and govern the dynamics after very short transients, even if most of the neural field has its initial condition in the attraction basin of the spatially homogeneous stable fixed point. The unconditional stability of the spatially homogeneous behavior is also recovered for values of Λ in the stationary region (D): the spatially homogeneous stationary state is attractive for the system with inhomogeneous initial conditions and the system converges towards a constant spatially homogeneous solution (see Fig. 7(c)).

For fixed values of Λ and a value of σ varying, the exact same type of instability of the spatially homogeneous equilibrium in region (A) and stability in regions (B)-(D) appears (see Figure 8). Similarly, instabilities in region (A) is characterized by irregular wave interactions. The main difference between the effects of Λ or σ lies in the fact that in the former case, the standard deviation of the solution of the mean-field equation has a constant value,

⁵We observed in our numerical simulations that the qualitative phenomena described do not sensitively depend on the choice of the initial condition.

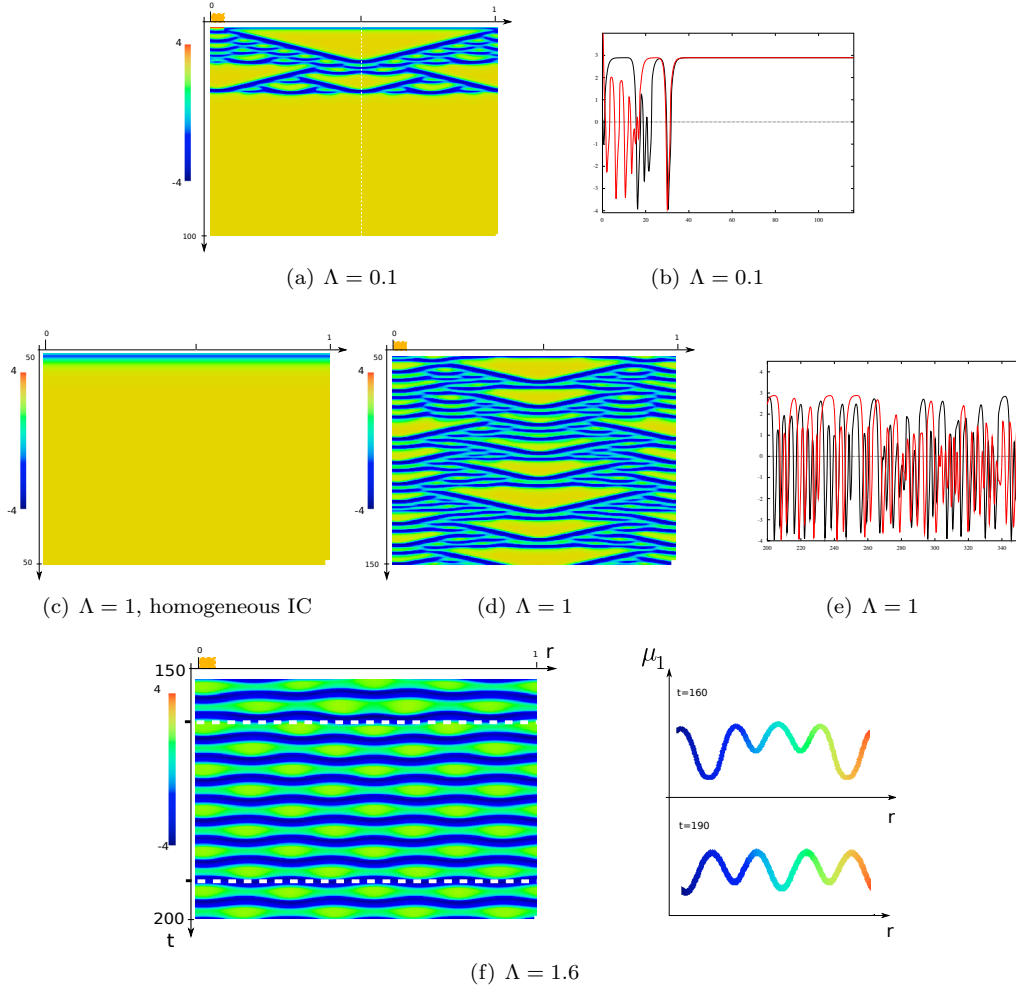


Figure 6: Irregular transient phases for inhomogeneous initial conditions, for parameters in region (A): $\mu_1(r, t)$ solutions of the two-layers mean-field equations is plotted. Spatio-temporal patterns: Abscissa: location on $\Gamma = [0, 1]$. Ordinate: time. Plots (b) and (e) represent $\mu_1(r = 0.1, t)$ (black) and $\mu_1(r = 0.5, t)$ (red). Initial conditions are set to $\mu_1(r, 0) = 5$ for $r \in [0, 0.05]$ and 0 elsewhere (orange box) $\mu_2(r, 0) \equiv 0$ and $v(r, 0) \equiv 0$, except in (c) where we show the solution for spatially homogeneous (null) initial conditions. (f): Space-time oscillation: $\Lambda = 1.55$. Waves no more interfere and the activity forms a non-stationary quasi-periodic structure. Right: plots of the activity for two different times as a function of $r \in \Gamma$. Animations of the activity are available in the supplementary material. Figures and animations were obtained using XPPAut [60].

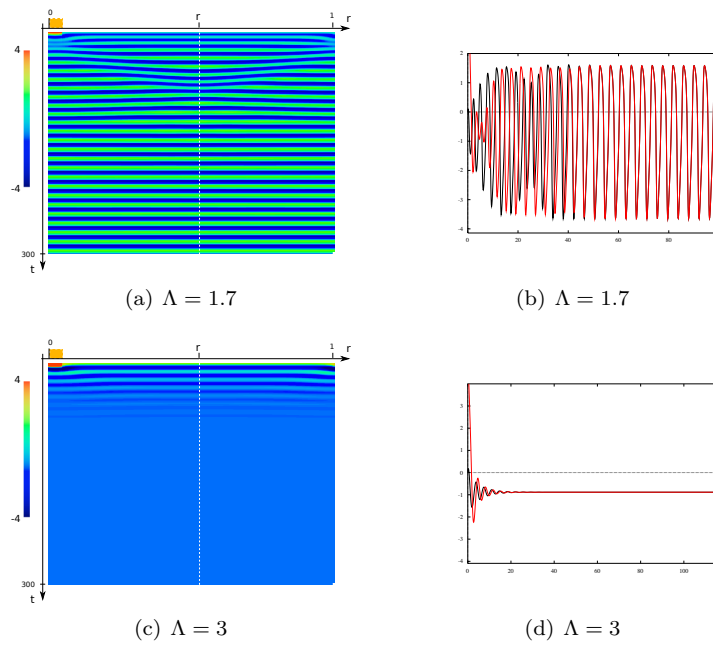


Figure 7: Spatially homogeneous stable behaviors: Λ belongs to the bistable (B), periodic (C) and stationary (D) regimes. Same inhomogeneous initial conditions and setting as in Fig. 6. Animations of the activity are available in the supplementary material.

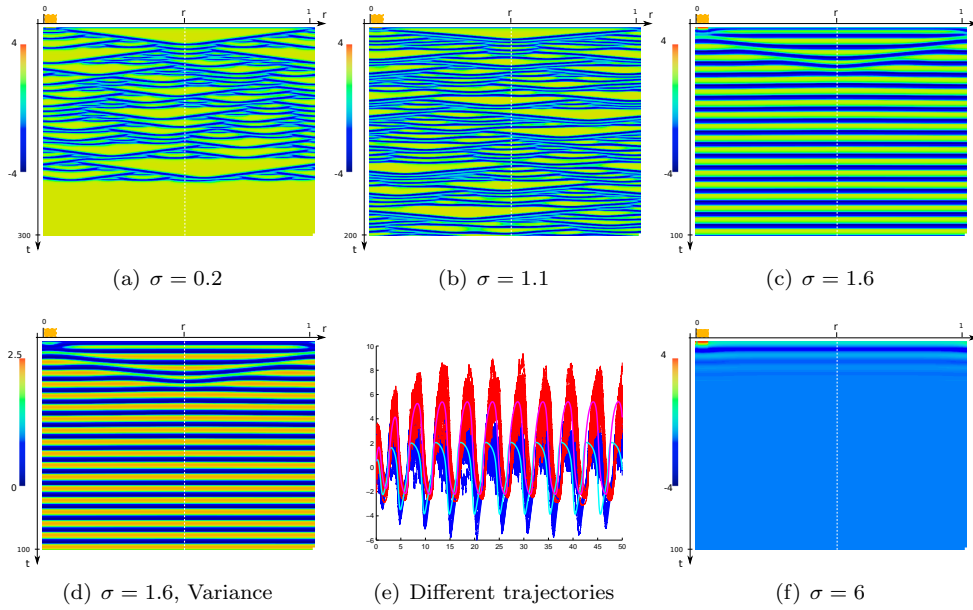


Figure 8: Behaviors of the two-layers mean-field equations for different initial conditions and synaptic noise amplitude σ . (e): 100 trajectories from the fully-synchronized equations stochastic equations in a network of 10 000 neurons show a sharp synchronization when the standard deviation reaches zero (blue: excitatory neurons (population 1) and red: inhibitory neurons (2)).

i.e. each individual trajectory in the network deviates from the mean activity by a Gaussian process with constant standard deviation, whereas in the latter case corresponds the standard deviation of the solution of the mean-field equations depends on the mean activity of the neural populations. This phenomenon is particularly visible in the non-stationary solutions. For instance for $\sigma = 1.6$, we observe that the standard deviation reaches very small values at times close to the onset of an oscillation, as shown in Figure 8(d), resulting in the fact that all neurons sharply synchronize at these times, a phenomenon particularly visible in the network simulations plotted in Fig. 8(e) where we plotted 100 trajectories of a network with 10 000 neurons.

All this analysis illustrate the fact that noise strongly shapes the form of the activity of large network, governing the nature of spatially homogeneous states, and their stability, yielding different spatio-temporal patterns that can be either transient or sustained. Irregular behaviors arose exclusively for relatively small values of the noise parameter, which again illustrates a stabilizing effect of noise in favor of the spatially homogeneous in law solutions. Very interesting irregular patterns of activity characterized by the irregular formation of waves and their splitting was observed in parameter regions close the presence of a saddle-homoclinic bifurcation in the fully synchronized system. This same phenomenon is found for similar systems defined on $[0, 1]$ with different boundary conditions: reflective or zero. Results are displayed in [Appendix B](#). This formation of complex spatio-temporal patterns arising from a wave-splitting phenomenon strongly evokes Turing patterns as found in different reaction diffusion equations in biological mathematics. In particular, these pat-

terns are similar to those exhibited by [61] and obtained from the analysis of the dynamics of reaction diffusion equations related to pattern formation on the shells of mollusks, in a case where the system induces the formation of forward and backward running waves that interact. These can be analyzed as done in [62] in a case where are identified self-replicating bumps, compared with dynamics observed dissipative equations such as Ginzburg-Landau's, but to our knowledge not observed in neural field equations. This structuring effect of noise and the presence of the particular type of spatio-temporal patterns observed in that system, beyond illustrating the fact that noise levels strongly shape the dynamics of neural fields.

Anatomical Connectivities: Bumps, bump-splitting and interfering waves. In this section we consider the anatomical case where distal interconnections are dominated by excitation and local interactions by inhibition. In that case, the codimension one bifurcation diagram of the synchronized system is provided in Figure 9(a) and shows the same global structure. This diagram characterizes the nature of spatially homogeneous solutions. We investigate solutions of the mean-field equations corresponding to non-homogeneous initial conditions, which, as observed in the previous sections, do not necessarily converge towards spatially homogeneous patterns.

The observations are essentially of the same kind as identified in the functional connectivity case. First of all, the bifurcation diagram of the spatially homogeneous equations can be segmented, like the previous case, into the same qualitative regions (A)-(D), and it appeared in that case again that the spatially homogeneous states were unstable only in the small noise region (A). However, we observed that depending on the ratio $r = s_1/s_2$, different kind of spatio-temporal patterns appeared (see Figure 9). For ratios greater than $r^* \approx 0.6$, the same phenomenon of wave splitting and interactions as in the functional case is observed (see Fig. 9(i)).

For $r < r^*$, a new type of dynamics appear, characterized by the presence of bumps of activity, i.e. localized stationary patterns. These are evidenced for initial conditions equal to zero except on an interval $[a, b] \in \mathbb{S}^1$. For $\Lambda = 1$, non spatially homogenous solutions appear, composed of a specific number of bumps that depends on the width of the interval $[a, b]$. As noise is increased, these bumps tend to split in two different bumps of the same spatial size and either stabilize, or split again, a phenomenon strongly evocative of the patterns observed in a different context by Coombes and Owen in [62]. This sequence of bump splitting can either stabilize into a stationary pattern composed of several bumps or appear repetitively depending on the value of the noise parameter. For relatively small noise values ($\Lambda < 1.7$), the activity stabilizes on a stationary pattern which is not spatially homogeneous, and the number of bumps and their shape depend both on the initial condition chosen and on the value of the noise. It is interesting to note that we observed that for $\Lambda > 1.5$, the stationary pattern found is spatially periodic, characterized by a specific wavenumber increasing as noise is increased, and depending on the type of initial condition chosen. For instance, we show in Figure 9(e) the case of $\Lambda = 1.5$ and initial condition zero except on $[0, 0.05]$ where it is equal to 5 (IC1), where the stationary behavior is characterized a spatially periodic pattern with wavenumber 8, and for initial condition zero except on $[0, 0.05] \cup [0.1, 0.15]$ where it is equal to 5, the same kind of phenomenon appears and stabilizes on a pattern with wavenumber equal to 9. For $\Lambda = 1.6$ and initial conditions IC1, the wave number is 10. For values of Λ larger than 1.7, the system no more stabilizes into stationary patterns and presents very complex irregular sequences of bump splitting, before presenting irregular spatio-temporal waves ($\Lambda = 2.2$, Fig. 9(i)).

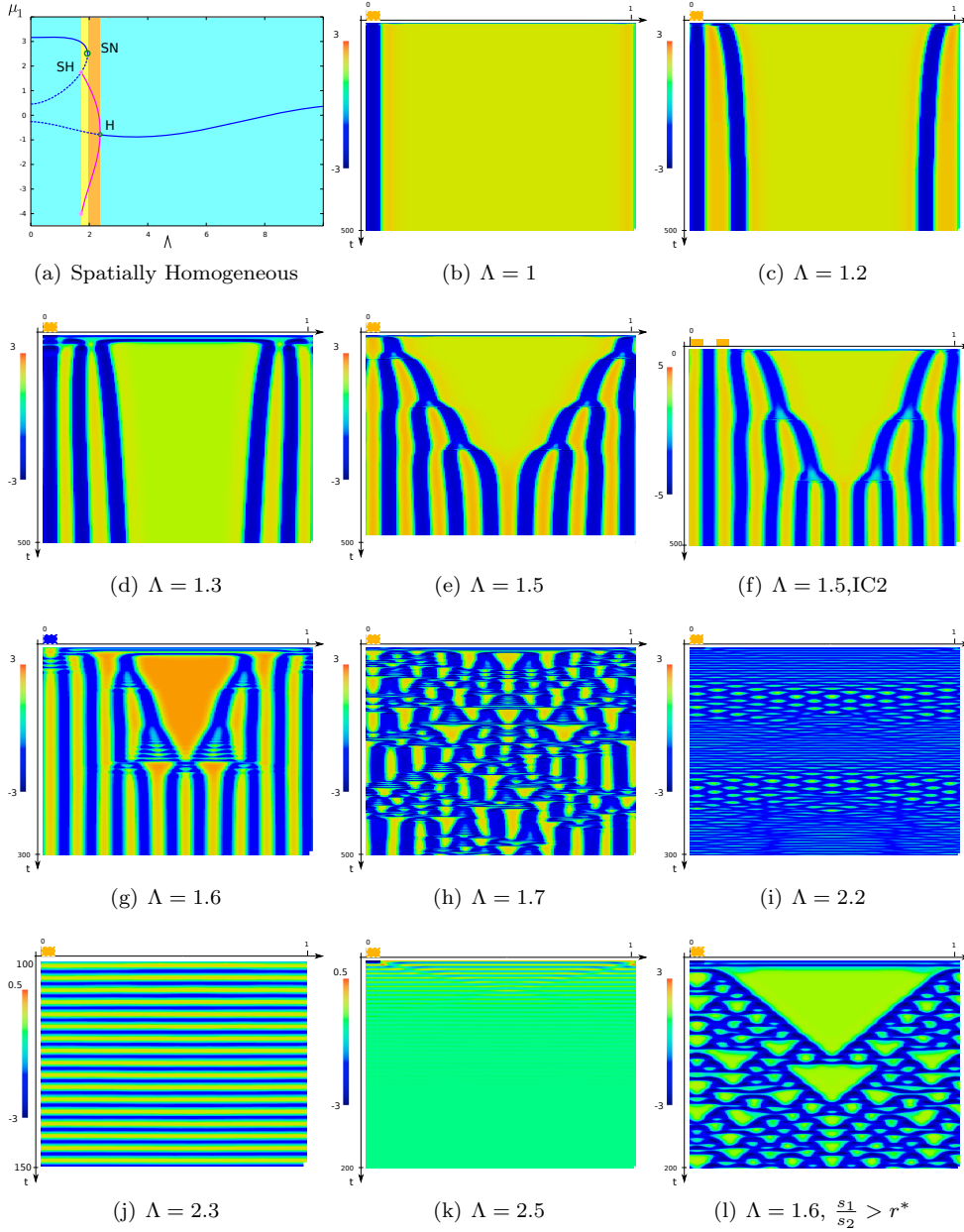


Figure 9: Anatomical connectivity case with $\mu_1(r, t)$ represented as a function of $r \in \mathbb{S}^1$ (abscissa) and t (ordinate). (a)-(k): $s_1/s_2 = 0.57$ show a sequence of bump splitting as Λ is increased in the parameter region where stationary spatially homogeneous solutions related to small values of Λ . Orange Box: initial condition $\mu_1(r, 0) = 5$ for $r \in [0, 0.05]$ and 0 otherwise, and blue box: $-\mu_1(r, 0)$. (l): $s_1/s_2 = 0.65$: wave splitting phenomenon, for $\Lambda =$

These bumps disappear in favor of a spatially homogeneous periodic activity when noise levels reach the bistable region, and this region turns into spatially homogeneous stationary solutions as noise is further increased, in the case corresponding to regions (B), (C) and (D).

For ratios s_1/s_2 greater than r^* , as stated, we find phenomena resembling to what was found in the functional connectivity case: for small values of the noise parameter, a wave-splitting and interference phenomenon is found, progressively turning into quasi-periodic spatio-temporal waves, spatially-homogeneous oscillations and spatially homogeneous stationary solutions as the noise is increased. The wave splitting phenomenon is displayed on Figure 9(1), other cases resemble to the other patterns found and are not displayed.

5. Discussion

In this article, we addressed the problem of characterizing the dynamics of large assemblies of neurons that are spatially extended and interact after delays. Modeling each individual neuron and characterizing their interactions, we derived neural field equations using a rigorous probabilistic mean-field theorem developed in [36]. The equations that were obtained in that article were implicit equations on stochastic processes probability distributions, and are extremely hard to tame in that general framework. We summarized the mathematical results obtained in a general setting, and provided a simple condition for the existence of solutions that are spatially homogeneous in law. The main result of the present article is the precise analysis of the dynamics of these equations in the particular case of firing-rate neurons, corresponding to the fact that membrane potential of the neurons have a linear intrinsic dynamics with nonlinear interactions. We were able in that case to reduce the mean-field equations to a set of delayed differential or integro-differential equations that are mathematically tractable, and using this description evidenced the important role of the microscopic noise in the dynamics in a series of examples of increasing complexity: finite-populations networks with delays, one-layer neural fields and two-layers neural fields. Several phenomena such as cascades of Hopf bifurcations, Turing-Hopf bifurcations and irregular spatio-temporal patterns were evidenced for specific levels of noise, and different levels of noise were identified corresponding to specific typical behaviors.

The first obvious limitation of the study is the fact that this precise analysis reduces to the case of firing-rate neurons. Though popular in the study of neural fields in the neuroscience community and widely used, this choice can be discussible in the present study. Indeed, the model does not take into account the highly nonlinear nature of several neuronal phenomena. This linear approximation is often seen as a heuristic mean-field limit itself, which can raise questions of the relevance of our present approach for neuroscience applications. The analysis developed here might hence better account for large-scale neuronal areas in which a very large number of cortical columns, described by the Wilson and Cowan model, interact. As far as neurons are concerned, we may add that a large body of experimental results have proved successfully accounted by linear dynamics, generally relative to the specific nonlinearly determined fixed point of normal brain activity. These linear models, though less general and accurate than the nonlinear ones, yielded much greater insight, and in particular analytic treatment, of the cortical dynamics within their regimes of validity. Probably the main reason why we chose this type of models is the reduction allowed by the Gaussian nature of the solutions. Indeed, as we demonstrated here, these models have the great advantage to be exactly and rigorously reducible to a set of tractable deterministic equations. This is hence a breach to go further in analyzing the complex dynamics of the

neural fields mean-field equations, with the aim of further understanding nonlinear neuron models. The analysis provided here is the first (and to our understanding, the only case where such an analytical study is possible) to address precisely the dynamics of such complex mean-field equations, and can also be seen as a proof of concept of the dynamics of this class of equations, in particular the effects of noise and delays in these equations. All these reasons motivated the investigation of linear models to uncover the dynamics of the more complex nonlinear neural fields models. We expect that nonlinear equations of this kind will also reveal other behaviors that are not reproduced in our linear approach. A perspective of great interest also would be to derive from the non-linear mean-field equations systems governing macroscopic variables such as the mean firing-rate. This is a complex and deep question we are currently investigating.

The general version of the results of theorems 1 and 2 have several implications in neuroscience that are discussed in [36]. Among these, we may recall that the propagation of chaos property implies an independence between the behavior of finite sets of neurons, a surprising property in the classical view of neural populations postulating that the activity of neurons belonging to the same neuronal population, since sharing common input and strongly interconnected, was highly correlated. This view was recently contradicted by several experimental articles that exhibited high quality data corresponding to extremely low levels of correlation, in the primary visual area V1 of awake macaques [10] and in the rodent neocortex [11]. These results confirm that the chaotic state is biologically relevant, and also have several implications in neural coding, as shown in the analysis of the coding efficiency of decorrelated activity in [10]. The independence of the neural activity also reconciles spike [9, 63] and rate [64] coding, two opposing conceptions of the neural activity, by emphasizing the role of collectivity: observing the state of several independent neurons during a time corresponding of the emission of a few spikes allows precise evaluation of the probability distribution of the interspike interval, hence the firing rate of neurons.

One of the main new feature of the mean-field model is the consubstantial integration of the noise in the dynamics of the neural field: in the reduced equations obtained for the linear systems, we observed that noise appeared as a parameter in the sigmoidal function transforming the voltage into a mean-firing rate. This property quantified precisely the effect of noise in the behavior of neural fields through our mean-field equations. We studied a finite-population mean-field model with delays, and showed noise and delays shape the behavior of the system. As delays are increased, a sequence of Hopf bifurcation appears in the system, that was observed numerically and accounted for analytically by the analysis of the characteristic roots for a particular system. This sequence of Hopf bifurcations produces complex transient behaviors, and simultaneously with noise levels shape the nature of the response of the neural field, by producing either stationary or oscillatory responses. Continuous neural fields were then analyzed with the particular aim of exhibiting qualitative changes in the behavior of a neural field due to noise levels. This is why we addressed the presence of Turing-Hopf bifurcations, first in a one-layer system semi-analytically, and then numerically in a more complex two-layers neural field. We evidenced several noise-induced dynamical Turing-Hopf bifurcations generating different spatio-temporal patterns, sometimes irregular and extremely complex. We also observed that noise also governs the stability of synchronized in law behaviors.

The periodic solutions triggered by an increase in the noise standard deviation correspond at the level of the network to solutions in which in neuron fires synchronously, in systems that present a unique stable fixed point when neurons are not driven by noise.

Noise hence appear to have a very strong structuring effect on the dynamics of the system, which can appear at first sight counterintuitive as noise is usually seen as altering the structure of the activity. These observations add to different phenomena documented in the neural networks literatures, as for instance coherent oscillations in neural networks [65, 66] where evidences for the presence of noise-induced in noisy integrate-and-fire neurons. The phenomena observed in our analysis differs from the more classical stochastic resonance or coherence resonance phenomena well documented in the neurocomputational literature (see e.g. [67] for a review of the effect of noise in excitable systems), since these correspond to the fact that there exists a particular level of noise maximizing the regularity of an oscillatory output related to periodic forcing (stochastic resonance) or to intrinsic oscillations (coherence resonance). Another important result that can be derived from the present analysis is the ability to define classes of parameter ranges attached to a few generic bifurcation diagrams as functions of the parameters. This property suggests model-based strategies for parameter evaluations in experimental measurements.

The present analysis, reducing noise levels to a simple parameter of a dynamical system, allowed going further into the analysis of the functional role of noise in the brain, a question currently widely debated in the neuroscience community, and relates this question to the presence of synchronized oscillations, as we showed in our different numerical simulations that noise levels determined the presence of oscillations, and the type of noise (additive or synaptic) the sharpness of the synchronization of oscillations across different neurons or areas.

Several extensions of the present study with applications in neuroscience and in applied mathematics are envisioned. The first would be, as already mentioned, to investigate similar phenomena in biologically relevant models and to study the behavior of the solutions of the mean-field equations in that mathematically much more complex setting that would include in particular nonlinear, excitable intrinsic dynamics and different ionic populations. The mean-field equations in that setting are complicated implicit stochastic equations, that can be written as a non-local nonlinear partial differential equation on the space of probability distributions. These equations are extremely hard to analyze directly, and the proof of concepts provided by this simpler analysis foreshadows interesting behaviors. An additional intricacy of the model is that, as we observed in our analysis, the system does not always present stationary solutions, and when these exist, they are not necessarily stable. Cycles were found, and bistable states between stationary and periodic behaviors were found, as well as irregular states in spatially extended systems. Analyzing the solutions of the non-linear mean-field equations will hence present interesting technical difficulties and probably complex behaviors, and necessitates the development of techniques to analyze the convergence of such stochastic equations towards periodic solutions. Another important direction in the development of this work would consist in fitting the microscopic model to biological measurements. This would yield a new neural assembly model for large scale areas and develop studies on the appearance of stochastic seizures and rhythmic activity in relationship with different parameters of the model, integrating the presence of noise in a mathematically and biologically relevant manner.

A question that remains largely open is the question of the number of neurons per population. Motivated by the fact that typical sizes of the neuronal populations are generally orders of magnitude larger than the number of neural populations (see e.g. [44]), we followed the choice made in [36] and assumed that the number of neurons in each population was increasing fast enough with the number of neurons (assumption of equation (3)), which left

room for the propagation of chaos to occur in each population. If this condition is not satisfied, different limits can appear, and characterizing these different limits is a challenging mathematical question. Another very interesting and deep question in this setting is the question of mean-field limits in slow-fast systems, problem that is highly relevant for different aspects of the neuronal behavior, and which raises a number of technical and applied questions.

Appendix A. Existence and Uniqueness of solutions of the synchronized mean-field solution

In this appendix we prove the existence and uniqueness of solutions of the fully synchronized system given by equations (7). This proof is similar to the proof given in [36]. Since the quantities $B(r, x, \varphi)$ and $H(r, x, \varphi)$ do not depend on r , we drop the dependence of these functions in r . As usually done, we transform the equation (7) into a fixed point equation on the space of stochastic processes. To this end, let us define the map Φ as follow:

$$\Phi(X)_t = \begin{cases} \zeta_0^0 + \int_0^t ds \left(G(s, X_s) + \mathbb{E}_Z[B(X_s, Z(\cdot))] \right) \\ \quad + \mathbb{E}_Z[H(X_s, Z(\cdot))] + \int_0^t dW_s g(s, X_s) & , \quad t > 0 \\ \zeta_t^0(r) & , \quad t \in [-\tau, 0] \\ (Z_t) \stackrel{\mathcal{L}}{=} (X_t) \in \mathcal{M} \text{ independent of } (X_t), (W_t(\cdot)) \text{ and } (B_t(\cdot, \cdot)) \end{cases}$$

The solutions of equation (7) are exactly the fixed points of Φ . We assume here that G and g are K -Lipschitz-continuous and satisfy the linear growth condition, and b and β are L -Lipschitz continuous in both their variables. It is easy to show that any possible solution has a bounded second moment following [36].

Existence:

Let $X^0 \in \mathcal{M}^2(\mathcal{C})$ such that $X^0|_{[-\tau, 0]} \stackrel{\mathcal{L}}{=} \zeta_0$ a given stochastic process. We introduce the sequence of probability distributions $(X^k)_{k \geq 0}$ on $\mathcal{M}(\mathcal{C})$ defined by induction as $X^{k+1} = (\Phi(X^k))$. We denote by (Z^k) a sequence of processes independent of the collection of processes (X^k) and having the same law. We decompose into six elementary terms the difference:

$$\begin{aligned} X_t^{k+1} - X_t^k &= \int_0^t \left(G(s, X_s^k) - G(s, X_s^{k-1}) \right) ds \\ &\quad + \int_0^t \mathbb{E}_Z \left[B(X_s^k, Z^k) - B(X_s^{k-1}, Z^k) \right] ds \\ &\quad + \int_0^t \mathbb{E}_Z \left[B(X_s^{k-1}, Z^k) - B(X_s^{k-1}, Z^{k-1}) \right] ds \\ &\quad + \int_0^t \left(g(s, X_s^k) - g(s, X_s^{k-1}) \right) dW_s \\ &\quad + \mathbb{E}_Z \left[H(X_s^k, Z^k) - H(X_s^{k-1}, Z^k) \right] \\ &\quad + \mathbb{E}_Z \left[H(X_s^{k-1}, Z^k) - H(X_s^{k-1}, Z^{k-1}) \right] \\ &\stackrel{\text{def}}{=} A_t + \tilde{B}_t + C_t + D_t + E_t + F_t \end{aligned}$$

where we simply identify each of the six terms A_t , \tilde{B}_t , C_t , D_t , E_t and F_t with the corresponding expression in the previous formulation. By a simple convexity inequality (Hölder) we have:

$$|X_t^{k+1} - X_t^k|^2 \leq 6 \left(|A_t|^2 + |\tilde{B}_t|^2 + |C_t|^2 + |D_t|^2 + |E_t|^2 + |F_t|^2 \right)$$

and treat each term separately.

The term A_t is easily controlled using Cauchy-Schwarz inequality, Fubini identity and standard inequalities and we obtain:

$$\mathbb{E} \left[\sup_{s \in [0, t]} |A_s|^2 \right] \leq K^2 t \int_0^t \mathbb{E} \left[\sup_{-\tau \leq u \leq s} |X_u^k - X_u^{k-1}|^2 \right] ds$$

Similarly, the martingale term D_t is bounded using the Burkholder-Davis-Gundy theorem to the d -dimensional martingale $(\int_0^t (g(s, X_s^k) - g(s, X_s^{k-1})) dW_s)$ and we obtain:

$$\mathbb{E} \left[\sup_{0 \leq s \leq t} |D_s|^2 \right] \leq 4K^2 \int_0^t \mathbb{E} \left[\sup_{-\tau \leq u \leq s} |X_u^k - X_u^{k-1}|^2 \right] ds$$

Let us now deal with the deterministic interaction terms \tilde{B}_t and C_t . We have:

$$\begin{aligned} |\tilde{B}_t|^2 &= \left| \int_0^t ds \int_{\Gamma} \lambda(r') dr' \int_{-\tau}^0 d\eta(r, r', u) (\mathbb{E}_Z [b(r, r', X_s^k, Z_{s+u}^k) - b(r, r', X_s^{k-1}, Z_{s+u}^k)] \right|^2 \\ &\leq t \lambda(\Gamma) \kappa \int_0^t ds \int_{\Gamma} \lambda(r') dr' \int_{-\tau}^0 d\eta(r, r', u) \mathbb{E}_Z [|b(r, r', X_s^k, Z_{s+u}^k) - b(r, r', X_s^{k-1}, Z_{s+u}^k)|^2] \\ &\leq t \lambda(\Gamma)^2 \kappa^2 L^2 \int_0^t |X_s^k - X_s^{k-1}|^2 ds \leq t \lambda(\Gamma)^2 \kappa^2 L^2 \int_0^t \sup_{-\tau \leq u \leq s} |X_u^k - X_u^{k-1}|^2 ds \end{aligned}$$

hence easily conclude that

$$\mathbb{E} \left[\sup_{s \in [0, t]} |\tilde{B}_s|^2 \right] \leq t \lambda(\Gamma)^2 \kappa^2 L^2 \int_0^t \mathbb{E} \left[\sup_{-\tau \leq u \leq s} |X_u^k - X_u^{k-1}|^2 \right] ds$$

and similarly

$$\mathbb{E} \left[\sup_{s \in [0, t]} |C_s|^2 \right] \leq t \lambda(\Gamma)^2 \kappa^2 L^2 \int_0^t \mathbb{E} \left[\sup_{-\tau \leq u \leq s} |X_u^k - X_u^{k-1}|^2 \right] ds$$

Eventually, the terms E_t and F_t use Burkholder-Davis-Gundy (BDG) inequality in place of Cauchy-Schwarz' together with similar arguments as used for \tilde{B}_t and C_t . Using the cylindrical nature of the Brownian motions $(B_t(r, r'))$, BDG inequality yields, for the term E_t (and similarly for the term F_t):

$$\mathbb{E} \left[\sup_{s \in [0, t]} |\Theta_s|^2 \right] \leq 4 \lambda(\Gamma)^2 \kappa^2 L^2 \int_0^t \mathbb{E} \left[\sup_{-\tau \leq u \leq s} |X_u^k - X_u^{k-1}|^2 \right] ds$$

for Θ_t equal to E_t or F_t . Putting all these evaluations together, we get:

$$\mathbb{E} \left[\sup_{s \in [0, t]} |X_s^{k+1} - X_s^k|^2 \right] \leq 6(T+4)(K^2 + 2\lambda(\Gamma)^2 L^2 \kappa^2) \int_0^t \mathbb{E} \left[\sup_{-\tau \leq u \leq s} |X_u^k - X_u^{k-1}|^2 \right] ds \quad (\text{A.1})$$

Moreover, since $X_t^{k+1} \equiv X_t^k$ for $t \in [-\tau, 0]$ by definition, we have, noting

$$M_t^k = \mathbb{E} \left[\sup_{-\tau \leq s \leq t} |X_s^{k+1} - X_s^k|^2 \right],$$

the recursive inequality $M_t^k \leq K'' \int_0^t M_s^{k-1} ds$ with $K'' = 6(T+4)(K^2 + 2\lambda(\Gamma)^2 + \kappa^2)$, which classically allows concluding on the existence and uniqueness of solutions.

Appendix B. Spatio-temporal patterns for one-dimensional neural fields with reflective or zero boundary conditions

In this appendix, we reproduce the results obtained in section 4.2.2 with different boundary conditions. The system considered is essentially the same, i.e. a two layers excitatory-inhibitory neural field with exponential connectivity kernels, and set the connectivity matrix as done in the main text. In section 4.2.2, the neural field was defined on \mathbb{S}^1 , i.e. characterized with convolutional interactions and periodic boundary conditions on the connectivity kernel. We now choose in the present section different boundary conditions: *reflective*, in which case the total synchronization conditions are satisfied, and *zero* boundary conditions, in which case no spatially homogeneous solution exists.

Appendix B.1. Reflective boundary conditions

In the case of a connectivity defined by an exponential connectivity kernel on $\Gamma = [0, 1]$ with reflective boundary conditions, the stationary solutions are the same as in 4.2.2 and their bifurcation diagram given in Fig. 5. Numerical simulation of the spatio-temporal activity of this neural field for non-homogeneous initial conditions and different values of the noise parameter Λ are displayed in Figure B.10. For small values of the noise parameter in the parameter region (A), the inhomogeneous initial conditions produce large amplitude waves that interact together, creating a transient complex structure of spatio-temporal activity that stabilizes on a fully synchronized stationary solution (i.e. constant in space and time). For slightly larger noise amplitude, this transient irregular phase takes over and produce sustained dynamic irregular activity on the neural field. As noise is further increased, a spatio-temporal periodic activity arises as the waves become faster and stop interacting. When the noise parameter reaches parameter regions (B) or (C), the spatially homogeneous oscillatory activity is recovered after a short transient. For noise levels in the parameter region (D), the whole neural field integrates fast the inhomogeneous initial condition and converges towards a spatially stationary activity.

Appendix B.2. Zero boundary conditions

In the case of zero boundary conditions of the connectivity kernel, the system does not fulfill the synchronization condition on the kernel given by equation (6). We analyze here the dynamics of this system for homogeneous initial conditions, and simulation results are displayed in Figure B.11. In that case, neurons at locations r close to the boundaries 0 and 1 receive less input than neurons far from the boundaries, and non-synchronized patterns are observed for any parameter values. We however make similar qualitative observations on the activity of the neural field. In details, for small noise intensities, the mean of the state of each neuron converge towards a constant value depending on its space location (see Fig. 11(a) for $\Lambda = 0.1$). As noise is increased, irregular spatio-temporal patterns of

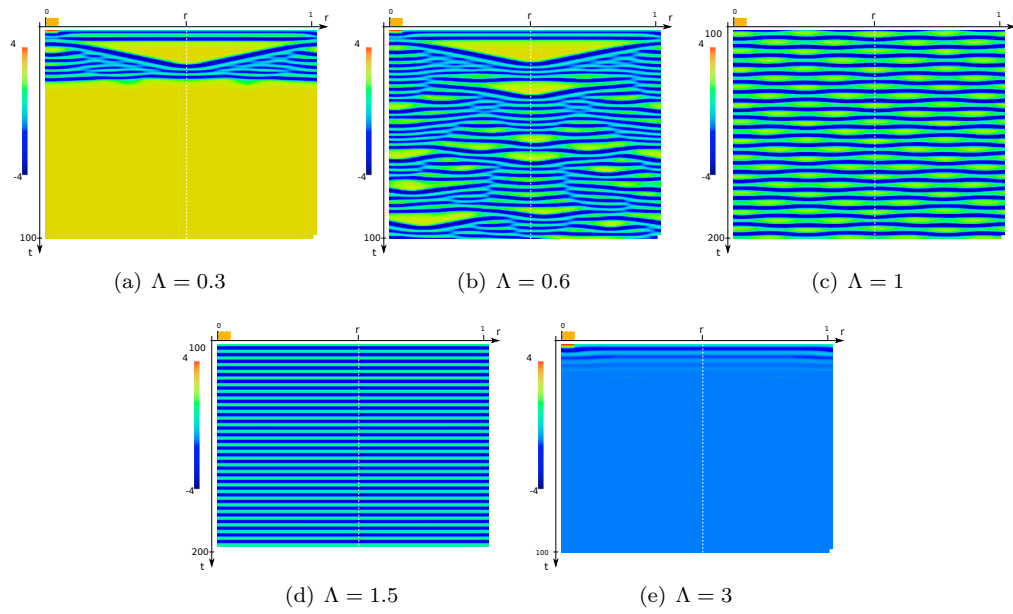


Figure B.10: Solutions of the mean-field equations for the reflective exponential connectivity kernel, as noise amplitude is increased. Abscissa represents the location on $\Gamma = [0, 1]$, Ordinate the time. Initial conditions are 5 on $[0, 0.025]$ (orange box) and else equal 0. Animations of the activity are available in the supplementary material.

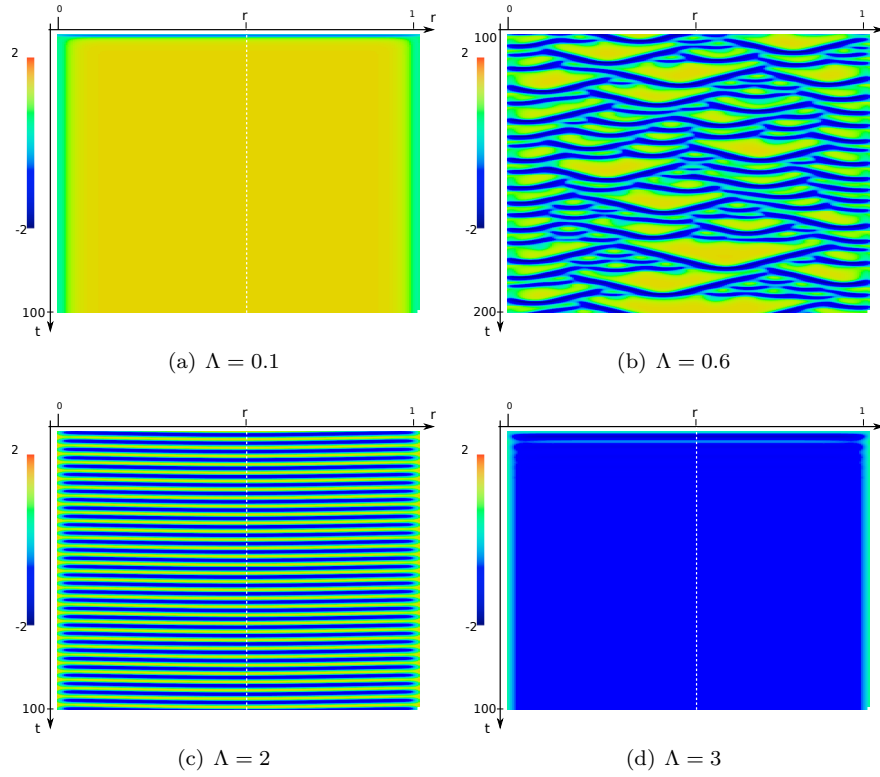


Figure B.11: Solutions of the mean-field equations for the exponential convolutional kernel with no (zero) boundary condition, as noise amplitude is increased. Abscissa represents the location on $\Gamma = [0, 1]$, Ordinate the time. Initial conditions are deterministic equal to 0. Animations of the activity are available in the supplementary material.

activity similar to these obtained in the previous cases are observed, and as noise increases this activity converges towards a periodic in time, non-synchronized activity that disappears into a constant in time, non-synchronized activity for larger values of the noise intensity. In this particular case, no transient irregular activity, nor spatio-temporal waves are found.

Acknowledgements

The author wants to warmly thank Romain Veltz for interesting technical discussions on the content and on relevant references, and David Colliaux for discussions on the choice of connectivity kernels. This work was partially supported by the ERC grant 227747, NerVi.

References

- [1] D. H. Hubel, T. N. Wiesel, M. P. Stryker, Anatomical demonstration of orientation columns in macaque monkey, *J. Comp. Neur.* 177 (1978) 361–380.

- [2] W. Bosking, Y. Zhang, B. Schofield, D. Fitzpatrick, Orientation selectivity and the arrangement of horizontal connections in tree shrew striate cortex, *The Journal of Neuroscience* 17 (6) (1997) 2112–2127.
- [3] T. Woosley, H. Van Der Loos, The structural organization of layer iv in the somatosensory region (si) of mouse cerebral cortex: The description of a cortical field composed of discrete cytoarchitectonic units, *Brain Research* (1969) 205–238.
- [4] E. Kandel, J. Schwartz, T. Jessel, *Principles of Neural Science*, 4th Edition, McGraw-Hill, 2000.
- [5] A. Roxin, N. Brunel, D. Hansel, Role of Delays in Shaping Spatiotemporal Dynamics of Neuronal Activity in Large Networks, *Physical Review Letters* 94 (23) (2005) 238103.
- [6] S. Coombes, C. Laing, Delays in activity based neural networks, Submitted to the Royal Society.
- [7] A. Roxin, E. Montbrio, How effective delays shape oscillatory dynamics in neuronal networks, *Physica D: Nonlinear Phenomena* 240 (3) (2011) 323–345.
- [8] P. Series, S. Georges, J. Lorenceau, Y. Frégnac, Orientation dependent modulation of apparent speed: a model based on the dynamics of feed-forward and horizontal connectivity in v1 cortex, *Vision research* 42 (25) (2002) 2781–2797.
- [9] S. Thorpe, A. Delorme, R. VanRullen, Spike based strategies for rapid processing., *Neural Networks* 14 (2001) 715–726.
- [10] A. Ecker, P. Berens, G. Keliris, M. Bethge, N. Logothetis, A. Tolias, Decorrelated neuronal firing in cortical microcircuits, *science* 327 (5965) (2010) 584. [doi:DOI:10.1126/science.1179867](https://doi.org/10.1126/science.1179867).
- [11] A. Renart, J. De la Rocha, P. Bartho, L. Hollender, N. Parga, A. Reyes, K. Harris, The asynchronous state in cortical circuits, *science* 327 (5965) (2010) 587.
- [12] G. Buzsaki, *Rhythms of the brain*, Oxford University Press, USA, 2004.
- [13] N. Tabareau, J. Slotine, Q. Pham, How synchronization protects from noise, *PLoS computational biology* 6 (1) (2010) e1000637
- [14] E. Izhikevich, Polychronization: Computation with spikes, *Neural Computation* 18 (2) (2006) 245–282
- [15] G. Ermentrout, J. Cowan, Large scale spatially organized activity in neural nets, *SIAM Journal on Applied Mathematics* (1980) 1–21.
- [16] S. Coombes, M. R. Owen, Bumps, breathers, and waves in a neural network with spike frequency adaptation, *Phys. Rev. Lett.* 94 (14).
- [17] R. Spreng, C. Grady, Patterns of brain activity supporting autobiographical memory, prospection, and theory of mind, and their relationship to the default mode network, *Journal of Cognitive Neuroscience* 22 (6) (2010) 1112–1123.

- [18] S. Amari, Characteristics of random nets of analog neuron-like elements, *Syst. Man Cybernet. SMC-2*.
- [19] S.-I. Amari, Dynamics of pattern formation in lateral-inhibition type neural fields, *Biological Cybernetics* 27 (2) (1977) 77–87.
- [20] H. Wilson, J. Cowan, Excitatory and inhibitory interactions in localized populations of model neurons, *Biophys. J.* 12 (1972) 1–24.
- [21] H. Wilson, J. Cowan, A mathematical theory of the functional dynamics of cortical and thalamic nervous tissue, *Biological Cybernetics* 13 (2) (1973) 55–80.
- [22] B. Ermentrout, Neural networks as spatio-temporal pattern-forming systems, *Reports on Progress in Physics* 61 (1998) 353–430.
- [23] G. Ermentrout, J. Cowan, Temporal oscillations in neuronal nets, *Journal of mathematical biology* 7 (3) (1979) 265–280.
- [24] C. Laing, W. Troy, B. Gutkin, G. Ermentrout, Multiple bumps in a neuronal model of working memory, *SIAM J. Appl. Math.* 63 (1) (2002) 62–97.
- [25] E. Rolls, G. Deco, *The noisy brain: stochastic dynamics as a principle of brain function*, Oxford university press, 2010.
- [26] L. Abbott, C. Van Vreeswijk, Asynchronous states in networks of pulse-coupled neuron, *Phys. Rev* 48 (1993) 1483–1490.
- [27] D. Amit, N. Brunel, Model of global spontaneous activity and local structured delay activity during delay periods in the cerebral cortex, *Cerebral Cortex* 7 (1997) 237–252.
- [28] N. Brunel, V. Hakim, Fast global oscillations in networks of integrate-and-fire neurons with low firing rates, *Neural Computation* 11 (1999) 1621–1671.
- [29] D. Cai, L. Tao, M. Shelley, D. McLaughlin, An effective kinetic representation of fluctuation-driven neuronal networks with application to simple and complex cells in visual cortex, *Proceedings of the National Academy of Sciences* 101 (20) (2004) 7757–7762.
- [30] T. Ohira, J. Cowan, Master-equation approach to stochastic neurodynamics, *Physical Review E* 48 (3) (1993) 2259–2266.
- [31] M. Buice, J. Cowan, Field-theoretic approach to fluctuation effects in neural networks, *Physical Review E* 75 (5).
- [32] M. Buice, J. Cowan, C. Chow, Systematic fluctuation expansion for neural network activity equations, *Neural computation* 22 (2) (2010) 377–426.
- [33] P. Bressloff, Stochastic neural field theory and the system-size expansion, Submitted (2009).
- [34] S. El Boustani, A. Destexhe, A master equation formalism for macroscopic modeling of asynchronous irregular activity states, *Neural computation* 21 (1) (2009) 46–100.

- [35] J. Touboul, G. B. Ermentrout, Finite-size and correlation-induced effects in mean-field dynamics finite-size and correlation-induced effects in mean-field dynamics, Arxiv preprint arXiv:1008.2839.
- [36] J. Touboul, Propagation of chaos in neural fields, (submitted).
- [37] A. Sznitman, Topics in propagation of chaos, Ecole d'Eté de Probabilités de Saint-Flour XIX (1989) 165–251.
- [38] Javier Baladron, Diego Fasoli, Olivier Faugeras, and Jonathan Touboul. Mean field description of and propagation of chaos in recurrent multipopulation networks of Hodgkin-Huxley and Fitzhugh-Nagumo neurons. *arXiv:1110.4294*, 2011.
- [39] J. Touboul, G. Hermann, O. Faugeras, Noise-induced behaviors in neural mean field dynamics, SIAM J. on Applied Dynamical Systems (in press).
- [40] G. Da Prato, J. Zabczyk, Stochastic equations in infinite dimensions, Cambridge Univ Pr, 1992.
- [41] X. Mao, Stochastic Differential Equations and Applications, Horwood publishing, 2008.
- [42] P. Chossat, O. Faugeras, [Hyperbolic planforms in relation to visual edges and textures perception](#), Plos Comput Biol 5 (12) (2009) e1000625. doi:doi:10.1371/journal.pcbi.1000625. URL <http://dx.doi.org/doi:10.1371/journal.pcbi.1000625>
- [43] G. Faye, P. Chossat, O. Faugeras, Hyperbolic bumps, in: Neurocomp (Ed.), Proceedings of the fifth French conference on Computational Neuroscience, 2010.
- [44] Y. Fregnac, M. Blatow, J. Changeux, J. De Felipe, A. Lansner, W. Maass, D. Mc Cormick, C. Michel, H. Monyer, E. Szathmáry, R. Yuste, Ups and downs in cortical computation, Microcircuits: the interface between neurons and global brain function, The MIT Press 393–433.
- [45] O. Faugeras, J.-J. Slotine, [Synchronizing a 2d continuum of two populations of neural masses](#), in: W. R. Holmes, R. Jung, F. Skinner (Eds.), Sixteenth Annual Computational Neuroscience Meeting (CNS), Vol. 8, Suppl 2 of BMC Neuroscience, 2007, p. 105. URL <http://www.cnsorg.org>
- [46] N. Venkov, S. Coombes, P. Matthews, Dynamic instabilities in scalar neural field equations with space-dependent delays, Physica D: Nonlinear Phenomena 232 (2007) 1–15.
- [47] S. Coombes, C. Laing, Delays in activity based neural networks, Philosophical Transactions of the Royal Society A. 367 (2009) 1117–1129.
- [48] J. Hale, S. Lunel, Introduction to functional differential equations, Springer Verlag, 1993.
- [49] R. Ben-Yishai, R. Bar-Or, H. Sompolinsky, Theory of orientation tuning in visual cortex, Proceedings of the National Academy of Sciences 92 (9) (1995) 3844–3848.
- [50] D. Hansel, H. Sompolinsky, Modeling feature selectivity in local cortical circuits, Methods of neuronal modeling (1997) 499–567.

- [51] K. Engelborghs, T. Luzyanina, D. Roose, Numerical bifurcation analysis of delay differential equations using dde-biftool, *ACM Transactions on Mathematical Software (TOMS)* 28 (1) (2002) 1–21
- [52] K. Engelborghs, T. Luzyanina, G. Samaey, Dde-biftool v. 2.00: a matlab package for bifurcation analysis of delay differential equations, Technical Report TW-330, Department of Computer Science, K.U.Leuven, Leuven, Belgium (2001).
- [53] R. Corless, G. Gonnet, D. Hare, D. Jeffrey, D. Knuth, On the lambertw function, *Advances in Computational mathematics* 5 (1) (1996) 329–359
- [54] L. Shayer, S. Campbell, Stability, bifurcation, and multistability in a system of two coupled neurons with multiple time delays, *SIAM Journal on Applied Mathematics* 61 (2) (2000) 673–700.
- [55] P. Bressloff, New mechanism for neural pattern formation, *Physical Review Letters* 76 (24) (1996) 4644–4647
- [56] A. Hutt, M. Bestehorn, T. Wennekers, Pattern formation in intracortical neuronal fields, *Network: Computation in Neural Systems* 14 (2) (2003) 351–368
- [57] R. Veltz, An analytical method for computing hopf bifurcation curves in neural field networks with space-dependent delays, *Comptes Rendus Mathematique* 1631-073X.
- [58] N. Venkov, [Dynamics of neural field models](http://www.maths.nottingham.ac.uk/personal/pmxnav/nikola_venkov_09_neural_fields_phd_thesis.pdf), Ph.D. thesis, University of Nottingham, uRL: http://www.maths.nottingham.ac.uk/personal/pmxnav/nikola_venkov_09_neural_fields_phd_thesis.pdf (2008).
URL <http://www.maths.nottingham.ac.uk/personal/pmxnav/nikolavenkov09-neuralfields-phdthesis.pdf>
- [59] V. Dragoi, M. Sur, Dynamic properties of recurrent inhibition in primary visual cortex: contrast and orientation dependence of contextual effects, *Journal of Neurophysiology* 83 (2) (2000) 1019
- [60] B. Ermentrout, *Simulating, Analyzing, and Animating Dynamical Systems: A Guide to XPPAUT for Researchers and Students*, Society for Industrial Mathematics, 2002.
- [61] H. Meinhardt, M. Klinger, A model for pattern generation on the shells of molluscs, *Journal of Theoretical Biology* 126 (1987) 63–89.
- [62] S. Coombes, M. Owen, Exotic dynamics in a firing rate model of neural tissue with threshold accommodation, *Contemporary Mathematics* 440 (2007) 123 0271–4132.
- [63] S. Thorpe, Spike arrival times: A highly efficient coding scheme for neural networks, *Parallel processing in neural systems and computers* (1990) 91–94.
- [64] P. Dayan, L. Abbott, *Theoretical Neuroscience : Computational and Mathematical Modeling of Neural Systems*, MIT Press, 2001.
- [65] J. Pham, K. Pakdaman, J. Vibert, Noise-induced coherent oscillations in randomly connected neural networks, *Physical Review E* 58 (3) (1998) 3610.

- [66] W. Nesse, A. Borisyuk, P. Bressloff, Fluctuation-driven rhythmogenesis in an excitatory neuronal network with slow adaptation, *Journal of computational neuroscience* 25 (2) (2008) 317–333
- [67] B. Lindner, J. Garcia-Ojalvo, A. Neiman, L. Schimansky-Geier, Effects of noise in excitable systems, *Physics Reports* 392 (6) (2004) 321–424